

**Development of Green Geopolymer Binders Utilizing
Blended Ladle Furnace Slag (LFS) with Metakaolin (MK)**

by

HAZIQAHT. S.HAMID

16811

Dissertation submitted in partial fulfilment of
the requirements for the
Bachelor of Engineering (Hons)
(Chemical Engineering)

MAY 2015

Universiti Teknologi PETRONAS
32610 Bandar Seri Iskandar
Perak Darul Ridzuan

CERTIFICATION OF APPROVAL

**Development of Green Geopolymer Binders Utilizing
Blended Ladle Furnace Slag (LFS) with Metakaolin (MK)**

by

Haziqah Binti S.Hamid

16811

A project dissertation submitted to the
Chemical Engineering Programme
Universiti Teknologi PETRONAS
in partial fulfilment of the requirement for the
BACHELOR OF ENGINEERING (Hons)
(CHEMICAL ENGINEERING)

Approved by,

(Dr. Nurlidia Bt. Mansor)

UNIVERSITI TEKONOLOGI PETRONAS

BANDAR SERI ISKANDAR, PERAK

MAY 2015

CERTIFICATION OF ORIGINALITY

This is to certify that I am responsible for the work submitted in this project, that the original work is my own except as specified in the references and acknowledgements, and that the original work contained here in have not been undertaken or done by unspecified sources or persons.

HAZIQAHT. S.HAMID

ABSTRACT

Geopolymer is defined as the chains of network of mineral molecules synthesized by a reaction of aluminosilicate mineral with alkali activator solution. It possesses good chemical and mechanical properties and has a great potential to be used in various application. The major aim of this research is to conduct a study on the geopolymer reaction utilizing blended ladle furnace slag (LFS) with metakaolin (MK) as a geopolymer precursor and the characterization of all the raw materials. The research focused on the relationship between of a series of samples with varying compositional ratios that was synthesized from a combination of LFS and MK. Setting time of fresh paste and compressive strength of hardened paste were determined using vicat needle test and compression machine respectively. For hardened paste, the mixes were cast in 50mm x 50mm x 50mm molds and the samples were cured in 60°C in the oven. The samples were examined after 7, 14 and 28 days in terms of porosity test, compressive strength test and degree of reaction. The characterization of chemical, mineralogical, physical characteristic, surface morphology and structural analysis of the particles was conducted by using various equipment such as XRF, FESEM, FTIR, XRD and Malvern Particle Size Analyzer. The results showed that LFS cannot be used on its own for geopolymerization process due to low content of Si/Al ratio. Higher loading of LFS causes higher porosity and reduces compressive strength. Therefore, the addition of MK was found to be necessary in order to improve compressive strength until the optimum level. The compressive strength however reduces after this point. It was observed that the best composition for binder was produced at a ratio of 50:50 ratio of LFS and MK (G-50:50). This formulation provided a consistent high compressive strength and slower setting time as well as the highest degree of reaction for a more convenient period of workability for application in construction or buildings.

ACKNOWLEDGEMENT

I would like to take this golden opportunity to firstly express my greatest gratitude to the people who played their role for the successful completion of the Final Year Project with the topic “Development of Green Geopolymer Binders Utilizing Ladle Furnace Slag (LFS) with Metakaolin (MK) ”. This grant is a part of a research collaboration between UTP and Southern Steel Sdn Bhd. Firstly, I would like to express our utmost gratitude to my supervisor, Dr. Nurlidia Bt. Mansor and also Prof Khairun for Final Year Project I and II. I would like to thank them for his continuous guidance and motivation throughout this project. They always willing to spare their time to see to my problem .Every single word and advice they shared with me has become the source of inspiration and motivation for driving me to move on towards a successful development of the final year project. Under their constant supervision, I managed to conduct the project with a proper planning until the completion of the projects according to the timeframe scheduled. This project has also won bronze medal at the 35th Science and Design Exhibition (SEDEX).

Apart from these, I would like to express my sincere thanks to our FYP Coordinators, Dr. Abrar Innayat and Dr. Nurul Ekmi for arranging various seminars for the final year students to enhance our knowledge in the methodology to conduct a proper research. Not to forget a special thanks to them for providing us sufficient time and guidance to ensure that we will be able to complete the final year project within the allowable timeframe.

In addition, I would like to express my special sense of gratitude to all the lecturers in Chemical Engineering Department for their continuous support and guidance throughout this project. I would like to thank my colleagues for providing their help, support and cooperation to ensure the success of this project. Last but not least, the appreciation goes to my parents, for their continuous support, motivation and encouragement which is the main driving force for me to strive hard to accomplish the

project despite all the challenges and hardships I faced during the completion of this project.

TABLE OF CONTENTS

CERTIFICATION OF APPROVAL	i
CERTIFICATION OF ORIGINALITY	ii
ABSTRACT	iii
ACKNOWLEDGEMENT.....	iv
TABLE OF CONTENTS	vi
LIST OF FIGURES	ix
LIST OF TABLES	xi
LIST OF ABBREVIATIONS.....	xii
CHAPTER 1: INTRODUCTION.....	1
1.1 Background.....	1
1.2 Problem Statement.....	2
1.3 Objective.....	3
1.4 Scope of Study.....	3
CHAPTER 2: LITERATURE REVIEW.....	4
2.1 Application Geopolymers	4
2.1.1 Geopolymer as a Cement.....	4
2.2 Geopolymer.....	5
2.2.1 Terminology and Chemistry	5
2.2.2 Raw Materials.....	7
2.2.3 Activator Solution.....	7
2.3 Characterization.....	8
2.3.1 Chemical Composition	8
2.3.2 Minerological Properties	8
2.3.3 Morphological Properties.....	9
2.4 Properties of Geopolymer.....	11

2.4.1	Compressive Strength.....	11
2.4.2	Setting Time	12
2.4.3	Porosity.....	12
2.5	Synthesis Parameters	13
2.5.1	Alkaline Concentration.....	13
2.5.2	Curing Temperature & Time	13
2.6	Degree of Reaction	15
CHAPTER 3:	METHODOLOGY / PROJECT WORK.....	16
3.1	Research Methodology	16
3.1.1	Raw Material Preparation&Alkaline Solution Preparation.....	16
3.1.2	Characterization of Raw Material and Geopolymer..	17
3.1.3	Determine the best solid to liquid ratio	18
3.1.4	Real samples preparation.....	19
3.1.5	Properties of Geopolymer.....	20
3.1.5.1	Setting time	20
3.1.5.2	Compressive Strength.....	21
3.1.6	Determination of Degree Of Reaction	22
3.2	Project Flowchart.....	23
3.2.1	Research method.....	23
3.2.2	Flow Chart Of Research Activities.....	24
3.3	Gantt Chart And Key Milestones.....	25
CHAPTER 4:	RESULTS AND DISCUSSION	27
4.1	Characterization Of Raw Materials	27
4.1.1	Chemical composition	27
4.1.2	Mineralogical properties.....	28
4.1.3	Morphological Properties	29

4.1.4 FTIR Analysis.....	33
4.2 Determination The Best Solid To Liquid Ratio.....	34
4.3 Experimental Result.....	38
4.3.1 Ray Diffraction (XRD).....	38
4.3.2 Morphological	41
4.3.3 FTIR Analysis.....	45
4.4 Physical Properties of Geopolymer.	47
4.4.1 Setting Time and Compressive Strength	47
4.4.2 Porosity Test	50
4.4.3 Degree of reaction	52
CHAPTER 5: CONCLUSION AND RECOMMENDATION	53
5.1 Conclusion.....	53
5.2 Recommendations	55
REFERENCE.....	56

LIST OF FIGURES

Figure 2.1	Conceptual model for geopolymerization	6
Figure 2.2	Raw material needed to produce cement	7
Figure 2.3	XRD of G-MK100,G-MK75,G-MK50,G-MK40,G-MK20 and G-LFS100	9
Figure 2.4	SEM Microgrphs of G-MK100 (a) , G-MK50(b) , G-MK-30 (c) and G-LS100	10
Figure 2.5	Compressive strength of investigated samples	11
Figure 2.6	Curing temperature & curing time vs compressive strength	14
Figure 3.1	Vicat apparatus	20
Figure 3.1 a-c	Steps measuring setting time	20
Figure 3.2	Compression machine	22
Figure 3.3	Research method	23
Figure 3.4	Flow Chart of research activities	24
Figure 4.1	XRD Pattern for raw LFS	28
Figure 4.2	XRD Pattern for raw MK	29
Figure 4.3	SEM Micrograph for Raw LFS	30
Figure 4.4	SEM Micrograph for Raw MK	30
Figure 4.5 a-b	The elements present in LFS	31
Figure 4.6 a-b	The elements present in MK	32
Figure 4.7	FTIR analysis for Raw LFS	33
Figure 4.8	FTIR analysis for Raw MK	34

Figure 4.9	Solid to Liquid Ratio vs Setting Time and Compressive Strength	37
Figure 4.10	XRD Pattern of Raw MK, G-MK100, G-25:75, G-50:50, G-75:25, G-LFS 100 and Raw LFS	40
Figure 4.11	Comparison of SEM Micrographs between Raw MK, G-MK100, G-25:75, G-50:50, G-75:25, G-LFS 100 and Raw LFS	43
Figure 4.12	Comparison of FTIR analysis between Raw LFS, G-LFS 100, Raw MK, G-MK100 and G-50:50	45
Figure 4.13	Setting time of samples prepared	48
Figure 4.14	Compressive strength of samples prepared	49
Figure 4.15	Porosity test	51
Figure 4.16	Degree of reaction	52

LIST OF TABLES

Table 2.1	Application of geopolymer	4
Table 2.2	Bulk composition (wt%) for both LFS and MK	8
Table 3.1	Activator solution used for geopolymerization	16
Table 3.2	Equipment used for characterization	18
Table 3.3	Mix-design of geopolymer paste and fixed parameter	19
Table 3.4	Gantt Chart and Key Milestone for FYP I and FYP II	25
Table 4.1	Chemical composition LFS and MK	27
Table 4.2	Solid to Liquid Ratio	35
Table 4.3	Porosity Result	36
Table 4.4	Detail of mixture proportions	37
Table 4.5	Structure of samples (Front and back view)	44
Table 4.6	Summary of main FTIR peak	46
Table 4.7	Setting time and compressive strength result	47
Table 4.8	Porosity result	50
Table 4.9	Degree of reaction (%)	52

LIST OF ABBREVIATIONS

LFS	Ladle furnace slag
MK	Metakaolin
AAM	Alkali Activated Materials
Si	Silica
Al	Alumina
CaO	Calcium Oxide
XRD	X-Ray Diffraction
XRF	X-Ray Fluorescence
FTIR	Fourier Transform Infrared Spectroscopy
SEM	Scanning Electron Microscopy
AAM	Alkali-Activated Materials
NaOH	Sodium hydroxide
Na ₂ SiO ₃	Sodium Silicate

CHAPTER 1

INTRODUCTION

1.1 Background

Steel slag is a by-product of steel making and steel refining processes (Yildirim & Prezzi, 2011). Basic oxygen furnace (BOF) and electric arc furnace (EAF) slags are slags produced during the separation of molten steel from impurities in steel-making furnaces. The slag occurs as a molten liquid melt and is a complex solution of silicates and oxides that solidifies upon cooling while the LFS is a byproduct from further refining molten steel after coming out of a BOF or EAF (Radenovic, Malina & Sofilic, 2013).

Knowledge of the chemical, mineralogical and morphological properties of steel slag is essential because several steel slags have beneficial properties such as good strength, durability and latent pozzolanic (cementitious) properties. All of these properties can be utilized in engineering applications, such as road construction, soil stabilization, as filler or binder in concrete or as drainage or low-permeability barrier layers (Andreas, Diener & Lagerkrist, 2014)

Due to the expanding of steel industry, waste as well as by-products from steel making are increasing. In Sweden and Europe, as much as 18% and 6% of the 1.4 and 17.6 million tons steelmaking slags respectively produced annually are landfilled (Andreas, et al. 2014). The same goes to fly ash (FA) which is an industrial by-product generated during the combustion of coal for energy production. In Thailand, from 3.0 million tons fly ash produced, 1.2 million tons are wastes discarded at landfill site (Chindaprasirt, Jaturapitakkul, Chalee & Rattanasak, 2009). Thus, the potential use of these materials as raw materials for green binder synthesis will be of great interest as well as providing a

greener option for waste disposal. Moreover, steel slag shows pozzolanic (cementitious) properties as well as MK.

The challenge in this work is to produce a green binder with a consistently high compressive strength and slower setting time for a more convenient period of workability for application in construction and buildings using LFS. However, an investigation into the characteristics of LFS proved that LFS is a weak cementing material (Ppayiani & Anastasiou, 2013) and show low content of Si/Al ratio but high content in CaO (Yildirim & Prezzi, 2011). These properties can be improved through geopolymer reaction in the presence of AAM. MK is ideally synthesized during the dehydroxylation of phase pure kaolin. MK can be the precursors for AAM since they contain high amount of alkali soluble Si and Al. LFS will be blended with MK to enhance and control the compositional, structural and morphological properties of the raw materials. Various process parameters will also be tested for best green binder performance. The results of this research are expected to provide extensive knowledge on the synthesis of this type of green binder system and ultimately unique properties of new generation of green binder based on local LFS-MK for optimum use in concrete or related structural applications.

1.2 Problem statement

In Malaysia, industrial and biomass wastes are being generated in large quantities. For example, Southern Steel Malaysia produces about 120,000 tons per year of electric arc furnace slag (EAF) and 20,000 -25,000 tons per year of LFS. These wastes are initially stockpiled in the steel plants and eventually sent to slag disposal sites. So recycling LFS to produce new materials such as a binder is a driving path towards promoting sustainable development can tackle this problem.

However the major problem and limitation for LFS to become a binder is due to its poor content of Si and Al content but high CaO. Therefore MK is used to balance the Si/Al content in making the geopolymer through geopolymerization process. In order to achieve the goal, AAM will be used during the experiment. MK can be the precursors for AAM due to their high content of Si and Al. By varying the composition of LFS and MK and fixing the curing time, concentration of NaOH and solid to liquid ratio, the setting time,

compressive strength, porosity and degree of reaction of the geopolymers will be investigated. By using AAM, it has been previously demonstrated that systems based on LFS and MK is able to form calcium-tich-alumino-silicate gels with impressive mechanical properties that can be used as a binder. (Bignozzi, Manzi, Lancellotti, Kamseu, Barbieri, Leonelli, 2012).

1.3 Objectives

The study of LFS as green geopolymer binder is done to meet the following objectives:

1. To characterize the raw materials LFS and MK.
2. To carry out the geopolymer reaction utilizing blended LFS/ MK.
3. To investigate and study the effects of synthesis parameters of the green binder derived from blended LFS/MK.

1.4 Scope Of Study

The scope of this study consists of characterizations and synthesis parameters of geopolymerization. This research will involve a collaboration between Southern Steel Malaysia and Universiti Teknologi Petronas (UTP). The objective is to produce green geopolymer binder by utilizing the sample of LFS from Southern Steel Malaysia with MK. The time frame to complete the research is approximately 8-9 months and will be conducted at Chemical, Civil and Mechanical Engineering laboratories in UTP.

Characterization will be carried out to characterize the raw materials and cured geopolymer .The concentration of NaOH, curing temperature and solid to liquid ratio are fixed at 8M, 60°C and 1.4 respectively. Geopolymers are cured for 7, 14 and 28 days and determined for setting time and compressive strength for fresh and hardened paste respectively as well as porosity and degree of reactions.

CHAPTER 2

LITERATURE REVIEW

2.1 Application Of Geopolymer

Geopolymeric materials have a wide range of applications in the field of industries such as automobile and aerospace, non-ferrous foundries and metallurgy, civil engineering and plastic industries. The type of application of geopolymeric materials is determined by the chemical structure in terms of the atomic ratio Si: Al. A low ratio of Si: Al of 1,2, or 3 initiates a 3D-Network that is very rigid while Si:Al ratio higher than 15 provides a polymeric character to the geopolymeric material. For many applications in the civil engineering fields, a low Si:Al ratio is suitable. Table 2.1 below show applications of geopolymeric materials based on silica to alumina atomic ratio (Davidovits, 1999)

TABLE 2.1. Application of geopolymer (Davidovits, 1999)

Si: Al Ratio	Applications
1	Bricks/Ceramics Fire protection
2	Low CO ₂ cements and concretes Radioactive and toxic waste encapsulation
3	Fire protection fibre glass composite Foundry equipments
>3	Sealants for industry, 200°C to 600°C Tooling for aeronautics SPF aluminium
20-35	Fire resistant and heat resistant fibre composites

2.1.1 Geopolymer as a cement

The development of geopolymer cement is an important step towards the production of environmentally friendly cements. Geopolymer is a type of amorphous alumino-silicate cementitious material. The geopolymer cement is produced by totally replacing the OPC. Therefore, the use of geopolymer technology not only substantially reduces the CO₂ emissions by the cement industries, but also utilizes the waste materials such as LFS which is one of the steel slag. For this project, it utilizes the MK and LFS. However, it is also noted that fly ash can be one of the possible sources for making geopolymer binders. Consumption of fly ash in the manufacture of geopolymer is an important strategy in making concrete more environmentally friendly. (Mustafa Al Bakri, Kamarudin, Bnhussain & Nizar, 2014)

2.2 Geopolymers

2.2.1 Terminology and Chemistry

The geopolymerization process involves a chemical reaction under alkaline condition on Si-Al minerals that result in a 3D polymeric chain and ring structure consisting of Si-O-Al-O bonds, as Figure 2.1 (Duxson, Fernandez-Jienez, Provis, Luckey, Palomo & Deventer ,2006) .

The proposed geopolymerization mechanism will include:

- i. dissolution of Si and Al from the raw materials in the alkaline solution
- ii. formation of mobile precursors(oligomers) of polymeric bonds Si-O-Si and/or Si-O-Al type
- iii. formation of geopolymeric framework through polycondensation of the oligomers and
- iv. hardening of the whole system to form an inorganic polymeric structure, comprising of mixtures of amorphous to semi-crystalline structure, at ambient or higher temperatures.

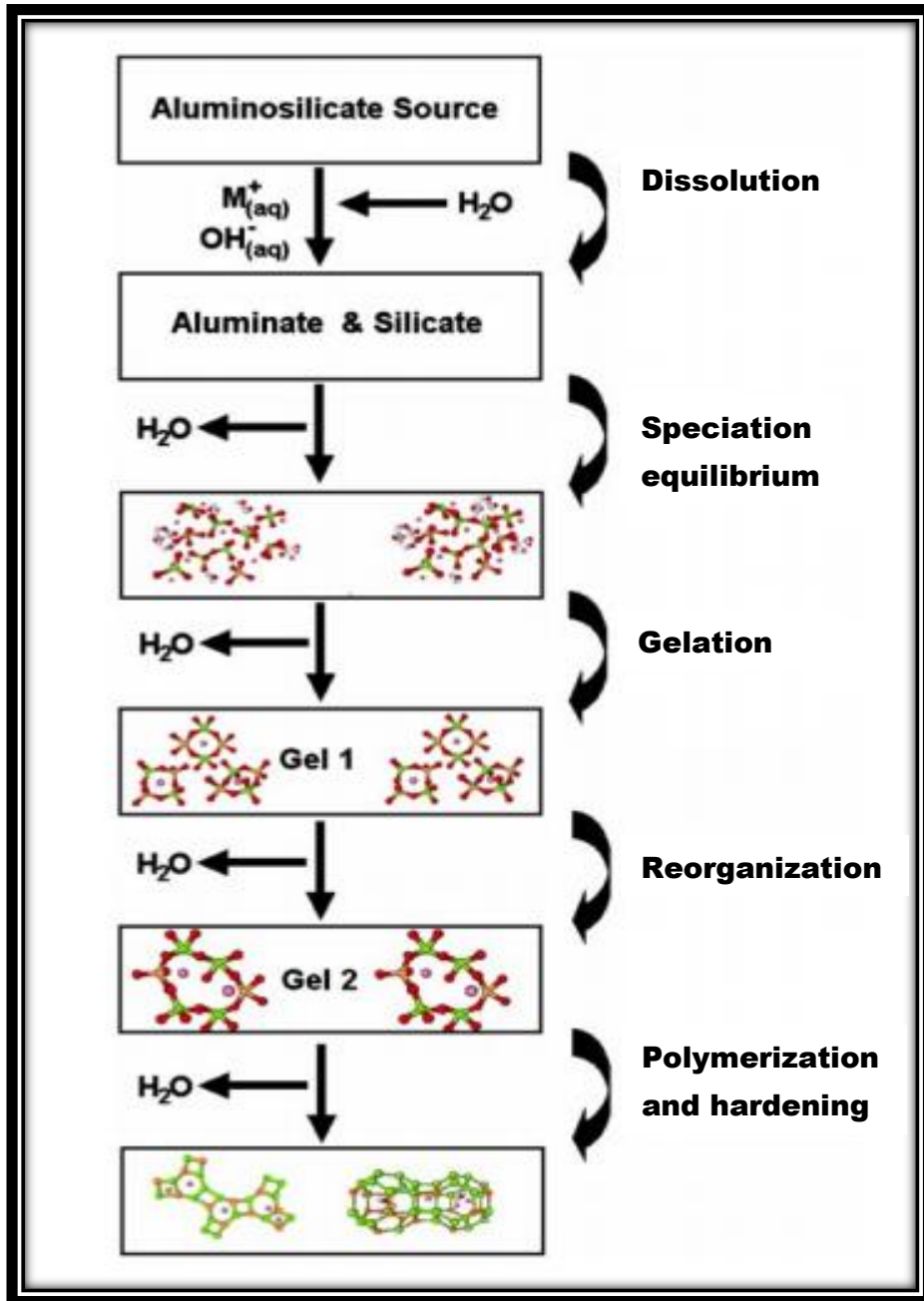


FIGURE 2.1. Conceptual model for geopolymerization (Duxson, Fernandez-Jienez, Provis, Luckey, Palomo & Deventer ,2006) .

2.2.2 Raw Materials

Raw materials plays an important role in the formation of geopolymer.

The ternary diagram in Figure 2.2 are the main raw materials needed to produce cement.

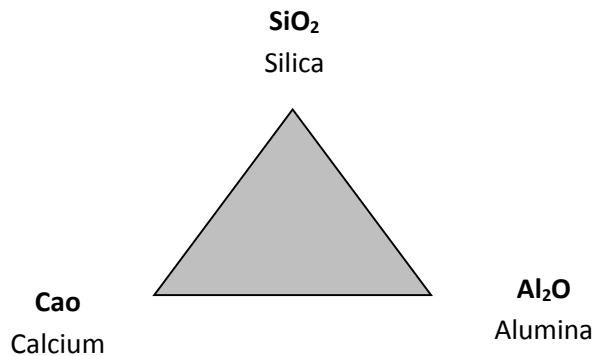


FIGURE 2.2. Raw material needed to produce cement (Hua Xu & Deventer 2000)

In this study, MK is used as the source of Al and Si to synthesis geopolymer. MK has higher reaction activation which can be derived from kaolinite which is a kind of artificial pozzolonic material. According to Hua Xu & Deventer (2000) , any pozzolonic compound or source of Si and Al that is readily dissolved in the alkaline solution acts as a source of geopolymer precursor species and thus lends itself to geopolymerization. Komnitsas & Zaharaki (2007) says that the mechanical strength can be improved by using MK due to decrement of water and salt transportation in the final product.

2.2.3 Activator Solution

Alkali (soluble base activator) and aluminate-rich materials are the source for alkali-activated cement to gain strength via chemical reaction. (Mustafa Al Bakri, et al. 2014) The alkali used as the activator tends to be an alkali silicate solution such as Na₂SiO₃ (waterglass) but can also be sodium hydroxide solution, or a combination of the two, or

other source of alkali. NaOH is require to dissolve the raw materials while Na₂SiO₃ will act as the activator for geopolymerization. The aluminate-containing material can be coal fly ash ash, MK, blastfurnace slag, steel slag or other slags, or other alumina-rich materials.

2.3 Characterization

2.3.1 Chemical Composition

The data shown in Table 2.2 shows the bulk composition (wt%) obtained for both LFS and MK by (Natali Murri, Rickard, Bignozzi, Van, 2013) using XRF. The result proved that the main constituent contribute in LFS is CaO but low Si and Al content compared to MK that contains the opposite composition. This is the reason why LFS usage as a binder is uncommon due to low Si/Al content which makes any research effort on this component difficult. Nevertheless this problem can be tackled by conducting geopolymerization process.

TABLE 2.2 Bulk composition (wt%) for both LFS and MK (Natali Murri, et.al. 2013)

Oxide	SiO ₂	Al ₂ O ₃	Fe ₂ O ₃	CaO	MgO	Others
LFS	17.9	13.0	7.1	42.1	6.1	3.8
MK	54.8	40.4	0.8	0.1	0.4	3.5

2.3.2 Mineralogical properties

The mineralogical properties of components can be determined by XRD. Based on the work of Bignozzi, et al. (2012) shown in Figure 2.3 the XRD of raw MK normally displays a broad hump at 22° 2θ which is still evident when geopolymerization occur at G-MK 100. However, when there are interaction between LS and MK during geopolymerization, the traces of MK peak are slowly disappear when decreasing the

content of MK. When the content of LS is increased, the peaks appear and become evident at 30-35 2θ .

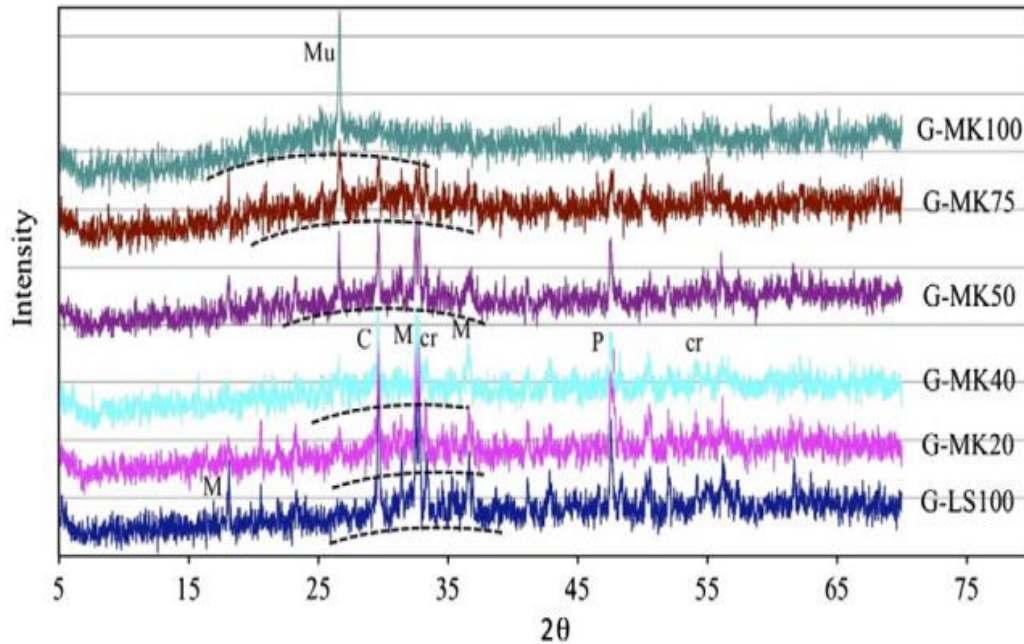


FIGURE 2.3. XRD of G-MK100,G-MK75,G-MK50,G-MK40,G-MK20 and G-LFS100 (Bignozzi, et al. 2012)

2.3.3 Morphological Properties

Microstructure investigation were carried out by Scanning Electron Microscopy (SEM) to determine the surface of raw LFS and raw MK and geopolymer samples after geopolymerization process take place. Based on Figure 2.4 studies by Bignozzi, et al. (2012) on G-MK 100 shows a very homogenous structure, characterized by the formation of Na-aluminosilicate (N-A-S-H) amorphous gel. By increasing the LS content, which particles are visible as white dots in SEM micrograph, the structure is grainy with different phases of arrangement comprising the inorganic polymeric matrix and some incompletely dissolved slag particles of small dimension around 10-30 μm .

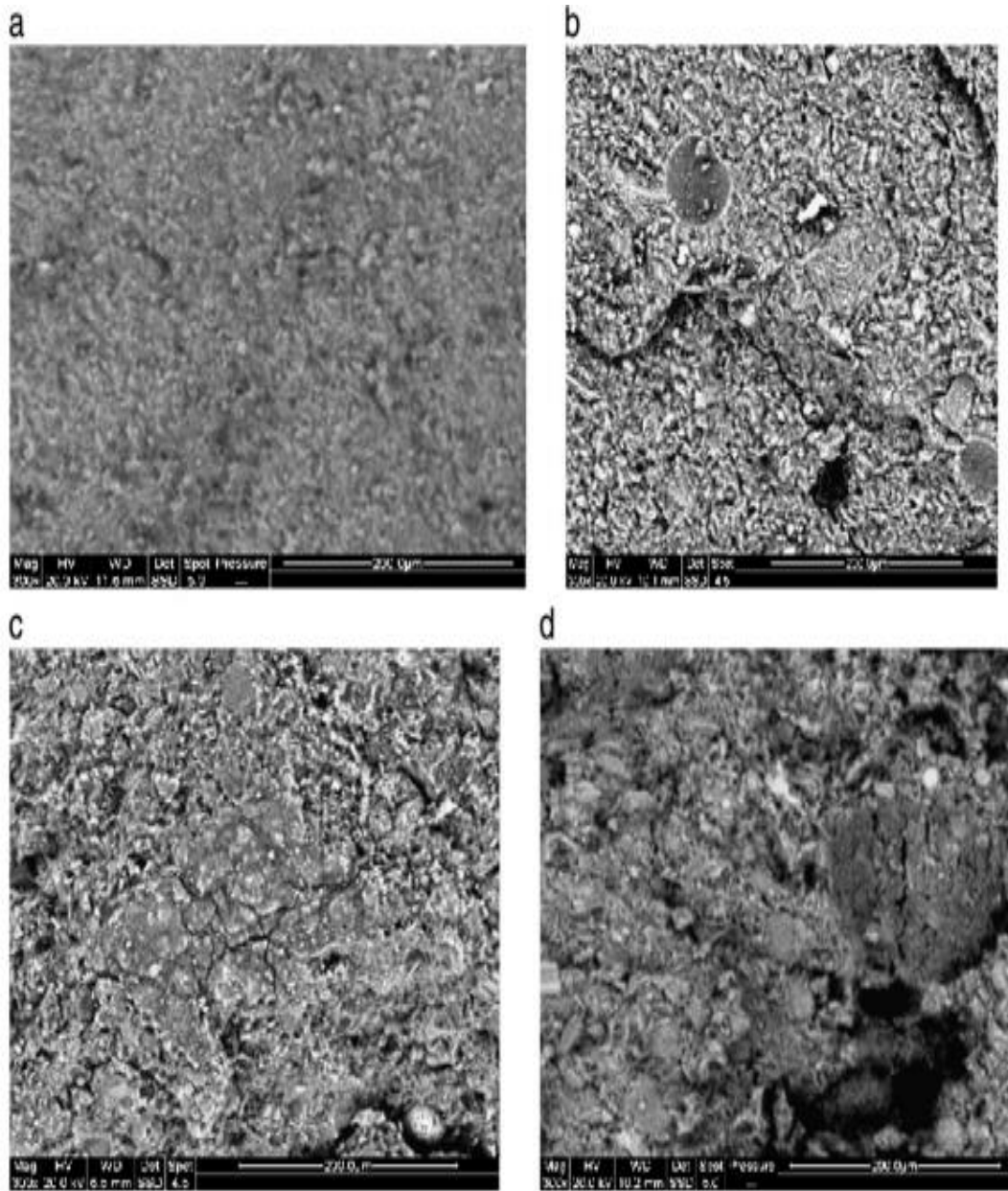


FIGURE 2.4. SEM Micrographs of G-MK100 (a) , G-MK50(b) , G-MK-30 (c) and G-LS100 Bignozzi, et al. (2012)

2.4 Properties Of Geopolymer

2.4.1 Compressive Strength

Once the composition is known, the proportions of LFS/MK can be varied in order to investigate the effect of different amounts of Ca, Si and Al in the alkaline activation process. Si plays the main role in geopolymerization in ensuring the strong bonds. Many researchers agree that the strength of material is enhanced by increasing the Si ratio, but after getting optimum compressive strength additional silica in the matrix can cause reduction in strength. (Fernandez-Jimenez, Ana & Palomo, 2005).

However, Bignozzi, et al. (2012) reported that with the increase of LFS content and decrease in MK content as shown in Figure 2.5 compressive strength grows reaching values in the range of 48-52MPa although LFS has low Si/Al ratio compared to MK. This contradicts with the studies of (Fernandez-Jimenez, et al. 2005). Therefore, further research is needed to confirm or support either findings.

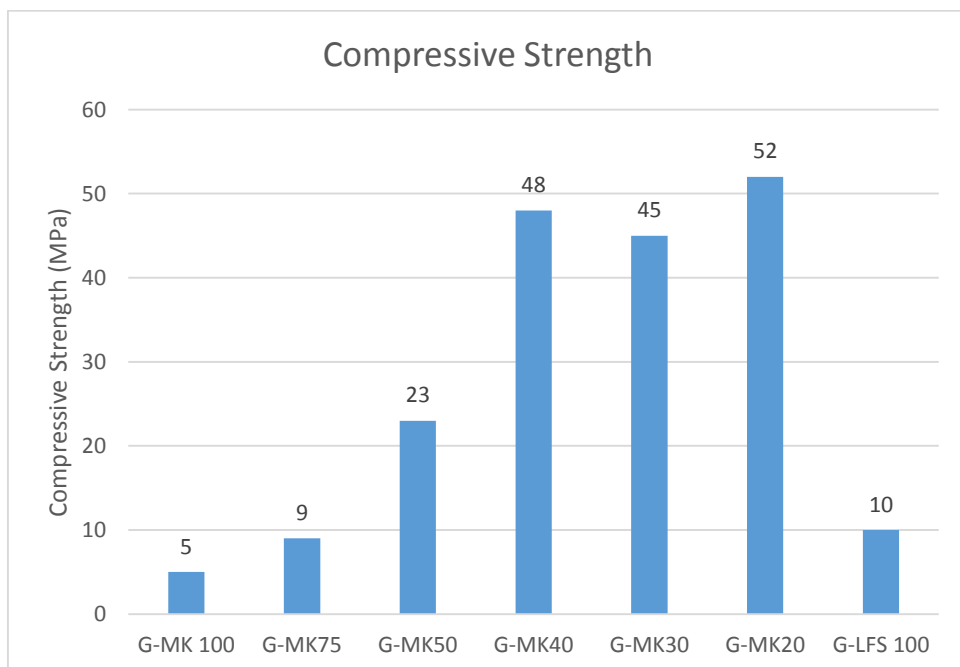


FIGURE 2.5. Compressive strength of investigated samples (Bignozzi, et al. 2012)

2.4.2 Setting Time

Setting time shows gradual reduction as higher solid to liquid ratio are used. Water content influenced setting time in the initial mixture. High reaction rate in greater solid to liquid ratio fasten the setting time of geopolymer. Activator liquid and MK content also effected the setting time of the mixture. MK mixture has been found to have significantly longer setting time as compared to control samples (Pantazopoulou, Tsivilis & Bagodiannis, 2004). Conversely, other researcher found MK to shorten setting times compared to other sample especially the control samples.(Maoulin, Blanc & Sorrentino, 2001). Moulin, et. Al (2001) said that a good binder should have a slower setting time for a more convenient period of workability for application in construction and buildings.

2.4.3 Porosity

Porosity can be defined as tiny holes that allow air, water, base and acid to pass through. That is the reason why porosity, particle size distribution play the most important role in the geopolymerization process especially in terms of compressive strength. A study reported by (Farhana F., Kamaruddin, Rahmat & Abdullah, 2014), the geopolymer paste samples at day 90 showed the highest compressive strength and lowest porosity while the geopolymer paste samples at day 7 showed the lowest compressive strength and highest porosity. For particle size distribution, when the size distribution is small, the porosity will become lower as it is harder for water or air to pass through the tiny holes and this will increase the compressive strength as well.

2.5 Synthesis Parameters

Geopolymerization depends on many factors including chemical composition of raw material, Si/Al ratio, Solid/Water ratio, Sodium Hydroxide (NaOH) concentration, water content, curing time and curing temperature (Temuujin, Williams & Riessen, 2009) that will affect the compressive strength of the binder.

2.5.1 Alkaline Concentration

There are many research conducted to study the effect of alkali concentration on compressive strength. The common alkaline activators used is sodium hydroxide (NaOH). The results from (Afshan A., Zakaria M., Khairun A., Nuruddin & Ismail, 2014) shows that 8M NaOH concentration gives high compressive strength as compared to 4M and 12M of NaOH. At low concentration (4M) of NaOH, the dissolution was low, less leaching of Si^+ and Al^{+3} took place and produced a material which had low compressive strength, whereas the drop in compressive strength at high concentration (12M) could be due to the large amount of Na^+ ion present in the cavities which prevent the formation of complete networks, Hence, the defect structure could be generated due the excess amount of Na^+ ion.

2.5.2 Curing Temperature and Curing Time

Curing time and curing temperature also play important role in geopolymerization because the water content is needed in the reaction. Most of the researches observed that increased in duration and temperature will produced a specimen with higher compressive strength.

Research from (Bing-hui, Zhu H., Cui, & Si Yu, 2014) from Figure 2.6 observed that 60 °C is the optimum curing temperature and recorded the highest compressive strength after 7days curing which is 97.95MPa. Increasing the curing temperature beyond 60°C will however decrease the compressive strength.

In terms of curing time, the longer the curing time, the higher the compressive strength. The compressive strength keep will increasing from 1 to 7 days due to the structure of samples becoming denser, harder and improve the crystallinity when the curing time is longer.

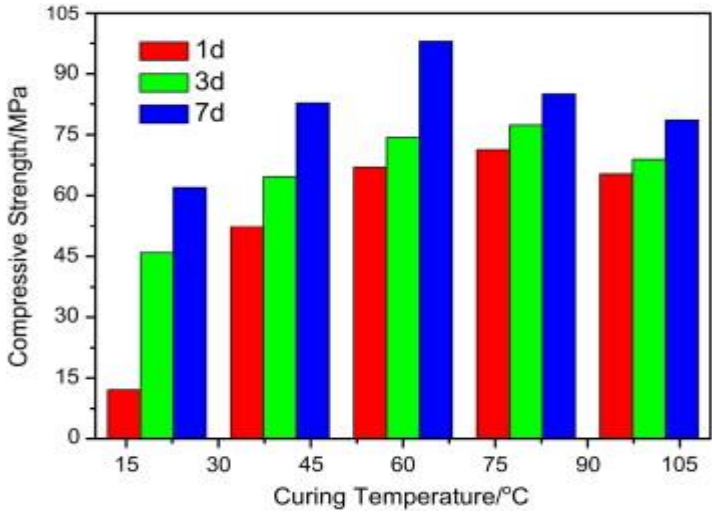


FIGURE 2.6. Curing temperature and curing time vs compressive strength (Binghui, et al. 2014)

A few tests have been carried out to observe whether LFS can produce as green binder as an OPC substitute or partial OPC substitute. The results from the test showed that LFS is a weak supplementary material that contains some hydraulic and pozzolonic properties. Therefore, it to improve is by finer material can be done either by sieving or by grinding (Ppayiani & Anastasiou, 2013).

2.6 Degree of Reaction

Geopolymerization consists of dissolution, speciation equilibrium, gelation, reorganization and polymerization steps as per discussed in 2.2.1. It is postulated that the last step, i.e., the polymerization, is the determining step for the strength of the resultant geopolymers. (Hua Xu, Jannie & Deventer, 2004) reported that only a high degree of polymerization can successfully stimulate the further dissolution and transfer of a substantial amount of Al and Si species from solid sources into the gel phase so as to increase the degree of geopolymerization. Moreover, the polymerization between Al and Si species may require a certain range of the Si-to-Al ratio in the gel, which could lead to a faster and a higher degree of reaction. Davidovits (1999) indicated that ideal geopolymers have molar Si/Al ratios of 1, 2, or 3 and that the geopolymers possessing a Si/Al molar ratio of 2 and containing both K and Ca gave the highest compressive strength with the highest degree of reaction.

According to Rahman & Kusbiantoro (2014), the degree of reaction was calculated by mass difference as follows:

$$\text{Degree of Reaction, } \varepsilon = (m_{\text{sample}} - m_{\text{residue}}) / m_{\text{sample}} \times 100\% \quad (1)$$

where m_{sample} is the weight of powdery sample in g ; m_{residue} is the weight of dried residue in g.

The amount of unreacted materials in geopolymer system will increase with lower reactivity of soluble silicate that prevent further dissolution of Al precursors and it will decrease the strength development of hardened specimens.

CHAPTER 3

METHODOLOGY / PROJECT WORK

3.1 Research Methodology

3.1.1 Raw material preparation and alkaline solution preparation

LFS which is a by-product of the steel making industry which was obtained from Southern Steel Berhad in Penang. MK was obtained from *Kaolin (M) Sdn Bhd* in Tapah, *Perak*. MK has to be calcined from commercial kaolin at 700°C for 6h. From (Elimbi, Tchakoute & Njopwouo, 2011) the compressive strength of hardened geopolymer cement paste samples recorded the highest compressive strength when calcined at 700°C for 6h. The LFS and MK were first sieved to 125µm.

Table 3.1 shows the activator solution used for geopolymerization and their function.

TABLE 3.1. Activator solution used for geopolymerization

Solutions	Description
Sodium hydroxide (NaOH)	<ul style="list-style-type: none">• Act as dissolver to activate Al and Si ions for geopolymerization• 8M NaOH was prepared by dissolving calculated amount of NaOH pellets in distilled water.
Sodium silicate (Na ₂ SiO ₃)	<ul style="list-style-type: none">• Pure Na₂SiO₃ was used to act as the activator for the geopolymerization

The activator solution, NaOH and Na₂SiO₃ were mixed together by fixing the weight ratio by 1:1. For example 50 g of NaOH were mixed with 50g of Na₂SiO₃ and leave it at least for 30minutes.

Molar mass of NaOH=40g/mol

$$(8 \text{ mol/L}) \times (1 \text{ L}) \times (40\text{g/mol}) = 320 \text{ g of NaOH pellets needed}$$

(2)

In the preparation of 8M NaOH solution, 320g of NaOH pellets was dissolved in distilled water in a 1L volumetric flask for 8M NaOH and the solution prepare at least one day before. Water is added to dissolve the solution and dilute to the calibration mark. It was then mixed well.

3.1.2 Characterization of Raw Material and Geopolymer

After preparing the raw material and alkaline solutions required for geopolymerization, the chemical, mineralogical and physical characteristics of all the raw materials were determined. Surface morphology and structural analysis of particles were also conducted. Various equipment such as XRF, XRD, FESEM, FTIR and Malvern Particle Size Analyzer will be used for characterization.

TABLE 3.2. Equipment used for characterization

Equipment	Description
XRF	For chemical analysis
XRD	To determine the mineralogical composition
FTIR	To obtain an infrared spectrum of absorption, emission, photoconductivity or Raman scattering of a solid, liquid or gas.
SEM	It is coupled with an energy dispersive X-ray (EDX) to analyze the morphological-microstructural of the samples.
Density meter	To check the density and porosity
Malvern Particle Size Analyzer	To analyze the particle size

3.1.3 Determine the Best Solid to Liquid Ratio

Three methods were carried out to find the best solid to liquid ratio before proceed to the real sample preparation.

Firstly, mixed LFS/MK (5g LFS + 5g MK) with activator solution (mixture of NaOH and Na₂SiO₃) that will form homogenous slurry. The best ratio will show the mixture that mix well.

Second method is by porosity test. Below is the formula to find porosity.

$$\text{Porosity} : (1 - d_b / d_t) \times 100\% \quad (3)$$

where:

d_b is bulk density

d_t is true density

Lastly is by determining the setting time of the sample for each ratio. Setting time which are too fast or too slow are not good geopolymer for binder application.

3.1.4 Real Samples Preparation

After all the tests above were carried out, the best solid to liquid ratio will be determined. By fixing the ratio, the study will proceed by varying the composition of LFS and MK. LFS and/or MK were mixed in a planetary mixer according to the formulation reported in Table 3.3 with the alkaline activator. Each mix is named with prefix G (for geopolymer) followed with LFS to MK by weight ratio, for example (for 100g solid ,25:75 represent 25g LFS and 75g MK) with the exception of the sample containing 100% LFS or 100% MK. After 5 minutes of mixing, the slurry were transferred in moulds to form prisms of 50mm X 50mm X 50mm and will be cured at 60⁰C for 7days, 14 days and 28days before testing for compressive strength for every composition of blended mixtures. The solid to liquid ratio and concentration of NaOH were fixed by 1.4 and 8M respectively. The setting time also will be taken into account for fresh paste using the Vicat apparatus (ASTM C191-08).

TABLE 3.3. Mix-design of geopolymer paste and fixed parameter

	LFS (g)	MK (g)
G-LFS 100	600	0
G-MK 100	0	600
G-25:75	150	450
G-50:50 (MK)	300	300
G-75:25	450	150

3.1.5 Properties of Geopolymer

3.1.5.1 Setting time Measurement for Fresh Paste

Setting time was measured using Vicat Apparatus as shown in Figure 3.1.



FIGURE 3.1. Vicat apparatus

Figure 3.1a, b and c are the methods to measure the setting time.

- Firstly, after mixing the paste, poured into the apparatus mould as shown in Figure 3.1a.
- Secondly, record the initial setting time by recording the time of a 1mm needle penetration in the softening specimen (Figure 3.1b).
- Finally, final setting time was determined by recorded the time of a penetration of 50mm needle until the needle unable sink visibly into the paste as shown in Figure 3.1c.
- So, the total time taken for the paste to reach it's harden state was measured as setting time.



Figure 3.1a



Figure 3.1b



Figure 3.1c

3.1.5.2 Compressive Strength Test for Hardened Paste

Compressive strength is defined as the capacity of the material to withstand the force applied to it. The material will crush as the force applied reach the limit of the compressive strength. This is the basic strength measurement method to determine the strength of the specimens.

After 7, 14 and 28 days curing at 60⁰C, compressive strength of geopolymer specimen was measured by the compression machine as shown in Figure 3.2. Cured geopolymer was placed in between of the upper and lower plate and the safety door was closed for safety purpose. The specimen was compressed until the yield stress was reached. The result shown in the indicator was recorded.



FIGURE 3.2. Compression machine

3.1.6 Determination Degree of Reaction

The reaction ratio of MK was determined by measuring unreacted MK stirring 1g of sample with 40 ml HCL(OH)₂ for 3 hours. The samples were then placed in centrifuge for 5 minutes with 7000rpm to separate solid from liquid. The centrifuge process is repeated by rinsing the sample with distilled water. The solid was then dried in the oven for 120⁰C for at least 4 hours. According to Alonso & Palomo (2001), the degree of reaction was calculated by mass difference as shown in equation 4. Any residue produced is the unreacted material.

$$\text{Degree of Reaction, } \varepsilon = (m_{\text{sample}} - m_{\text{residue}}) / m_{\text{sample}} \times 100\%$$

(4)

where $m_{\text{sample}} = 1 \text{ gram}$

Preparation of HCL(OH)₂ :

The preparation of HCL(OH)₂ was done by using a ratio of 1:20 of HCL to water. For example to prepare 40ml of HCL(OH)₂, 1.91ml of HCL and 38.1ml of water are needed and the solution mixed well.

3.2 Project Flowchart

3.2.1 Research method

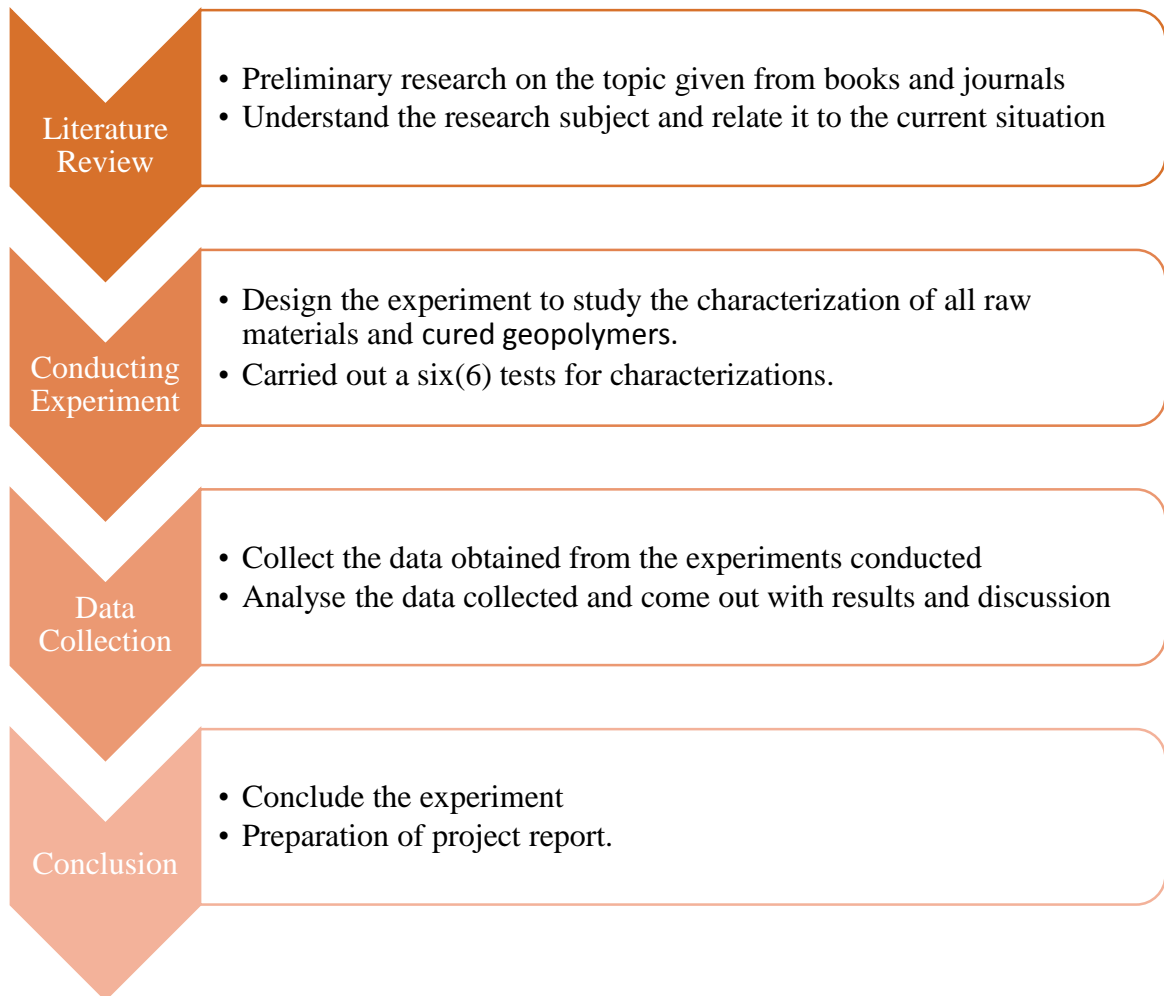


FIGURE 3.3. Research method

3.2.2 Flow Chart Of Research Activities

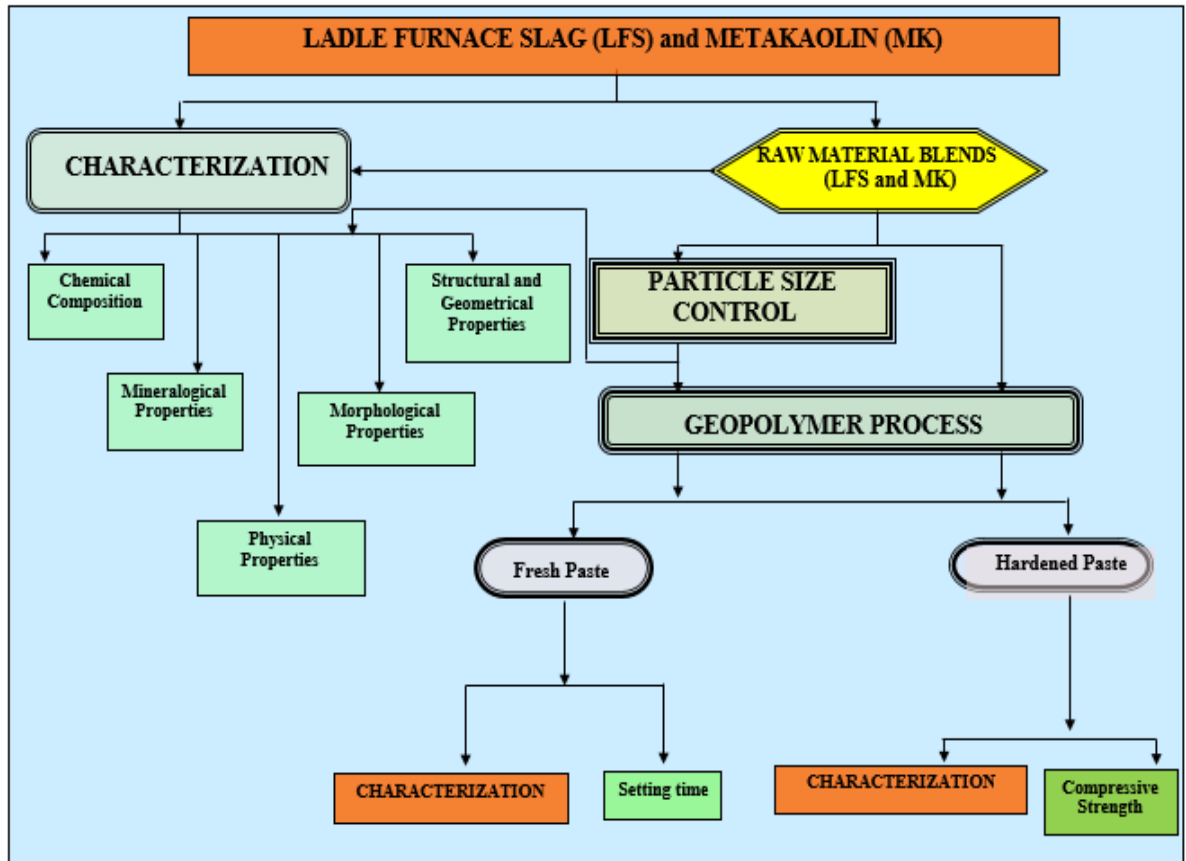


FIGURE 3.4. Flow Chart of research activities

3.3 Gantt Chart and Key Milestones for FYP I and FYP II

TABLE 3.4. Gantt Chart and Key Milestone for FYP I and FYP II

• **FYP I**

	1	2	3	4	5	6	7	8	9	10	11	12	13	14
Selection of Project Title	X													
Preliminary Research Work and preparing proposal														
Checking Equipment and Raw Materials					X									
Submission of First Draft of Extended Proposal						X								
Submission of Extended Proposal								X						
Proposal Defense Presentation									X					
Experimental work commences <ul style="list-style-type: none"> • Preparation of raw materials and alkaline solution activator • Do characterization for all raw materials 														
Submission of Interim Report-First Draft											X			
Submission of Interim Final Report													X	
Submission of marks by supervisors														X

• **FYP II**

	1	2	3	4	5	6	7	8	9	10	11	12	13	14	15
Determine the best solid to liquid ratio															
Preparation of samples with different composition and curing for 7days, 14days, 28days															
Test for setting time, compressive strength and Do characterization for 7days and 14days cured geopolymer samples															
Analyzing data and Preparation for Progress Report Submission															
Submission of Progress Report								X							
Project Work Continues • Test for setting time, compressive strength and do characterization for 28days cured geopolymer samples															
Pre-SEDEX											X				
Submission of Draft Final Report												X			
Submission of Dissertation (soft bound)													X		
Submission of Technical Paper													X		
Oral presentation														X	
Submission of Project Dissertation (Hard Bound)															X

CHAPTER 4

RESULTS AND DISCUSSION

4.1 Characterization of Raw Materials

4.1.1 Chemical composition

The chemical composition of the raw materials LFS and MK were determined by X-ray fluorescence spectrometry (XRF) on a dry sample basis.

TABLE 4.1. Chemical composition LFS and MK

Component	Chemical Composition Mass(%)	
	LFS	MK
SiO₂	18.5	53.6
Al₂O₃	2.46	41.7
Fe₂O₃	2.74	1.6
CaO	70.4	<0.1
MgO	1.99	-
SO₃	1.61	-
P₂O₅	0.672	-
MnO	0.604	0.11

TiO₂	0.556	1.70
ZnO	0.145	-

From the Table 4.1, LFS showed a high content of CaO with a certain amount of MgO, SiO₂, Al₂O₃ and Fe₂O₃ while MK was mainly constituted by SiO₂ and Al₂O₃ and also a small amount of others elements such as CaO. The XRF result showed the similar result that reported by A.Natali Murri, et al. (2013) as per discussed in the 2.3.11. It is proved that LFS has low content of alumina and silica but high content of CaO compared to MK. For the geopolymerization process as per discussed in 2.2.1 by P.Duxson, et al. (2006) which was that the first step involved the dissolution of Si and Al from the raw materials in alkaline solution. LFS cannot be used on its own for geopolymerization process and have to be mixed with MK as a precursor due to low content of Si and Al.

4.1.2 Mineralogical properties

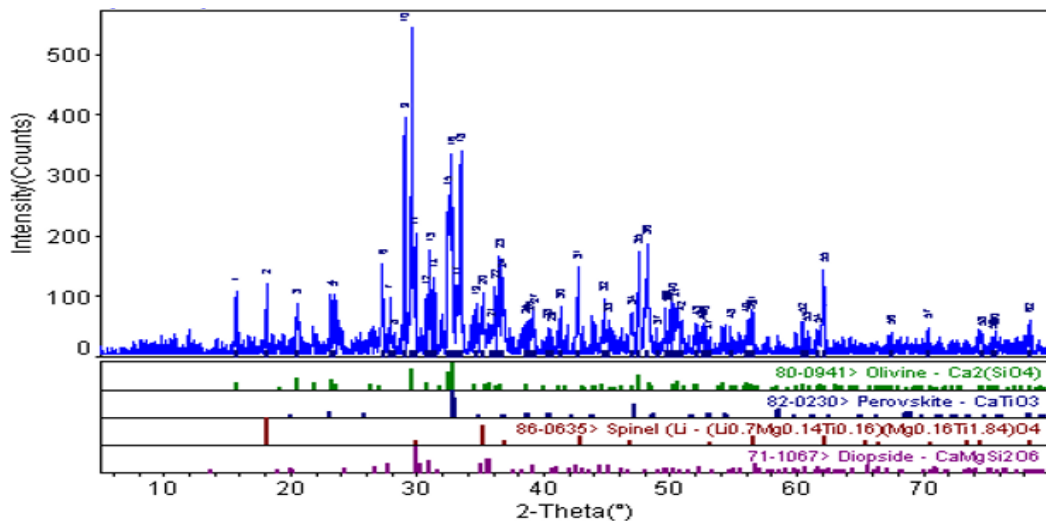


FIGURE 4.1. XRD Pattern for raw LFS

In Figure 4.1 for raw LFS , the major compound presents are calcium silicates (with or without small quantities of aluminium or magnesium) such as Diopside (CaMgSi₂O₆)

and olivine (Ca_2SiO_4). Aluminates such as spinel was present due to alumina contents in the slag. Other significance phase was such as perovskite (CaTiO_3), periclase (MgO) and iron oxide (Fe_xO_y). Ladle slag showed cementitious property mainly in the presence of an alkaline activator. The compound presents in G-LFS 100 were calcium aluminium silicate hydrates ($\text{CaAl}_2\text{Si}_7\text{O}_{18}\cdot 5\text{H}_2\text{O}$), yugmaralite ($\text{Ca}_4\text{Al}_7\text{Si}_{20}\text{O}_{18}$) and heulandite ($\text{CaAl}_2\text{Si}_7\text{O}_{18}\cdot 6\text{H}_2\text{O}$).

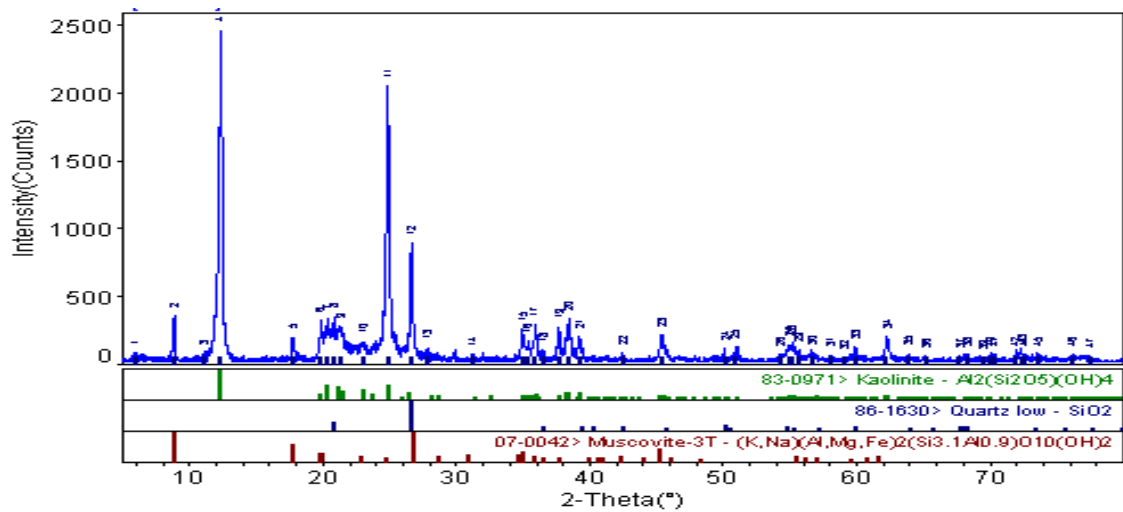


FIGURE 4.2. XRD Pattern for raw MK

As previously discussed, kaolin will be transformed to MK after calcined. The XRD pattern of calcined kaolin shows an amorphous pattern. However from Figure 4.2, there are still kaolinite peaks [$\text{Al}_2(\text{Si}_2\text{O}_5)(\text{OH})_4$] that showed that the calcination process was not complete. Quartz [SiO_2] and Muscovite [$(\text{K},\text{Na})(\text{Al},\text{Mg},\text{Fe})_2(\text{Si}_{3.1}\text{Al}_{0.9})\text{O}_{10}(\text{OH})_2$] were largely unreactive and remained in the metakolin.

4.1.3 Morphological Properties

There were two methods used to determine morphological properties. Firstly, LFS and MK particle size were analyzed using a laser particle-size analyzer. The particle size of LFS and MK were $18.279\mu\text{m}$ and $7.404\mu\text{m}$ respectively. It is differ from size that

recorded from Y.M Liew, H. Kamarudin, M. Al Bakri & M. Luqman (2012) which were found less 15 μm for LFS and 2 μm for MK. Smaller size will lead to higher dissolution of raw materials with alkaline solutions and give a greater compressive strength.

Four different magnifications used to analyze the shape of the samples which were 500x, 1000x, 1500x and 3000x respectively. From Figure 4.3 and Figure 4.4, the difference between LFS and MK particle sizes were clearly evident which were 18.279 μm and 7.404 μm respectively where the angular shape of LFS shown was bigger that MK.

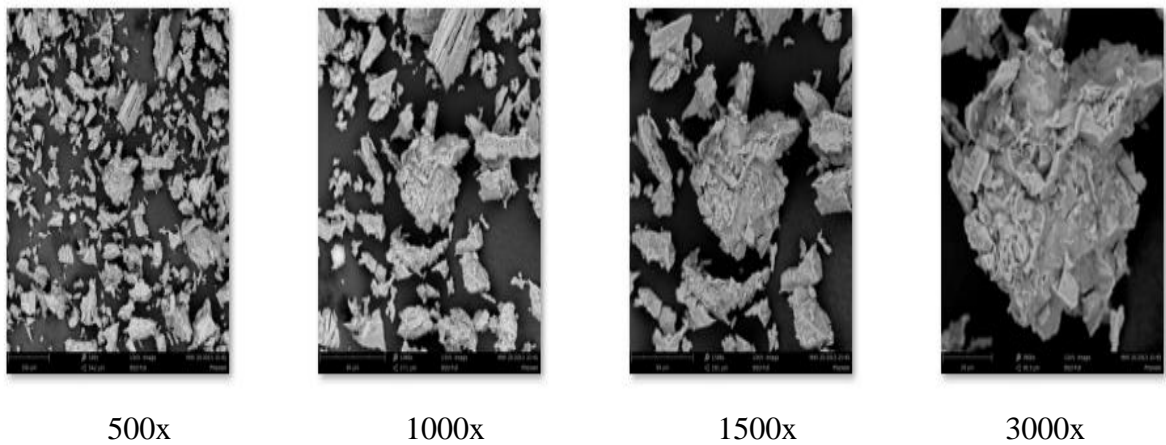


FIGURE 4.3. SEM Micrograph for Raw LFS

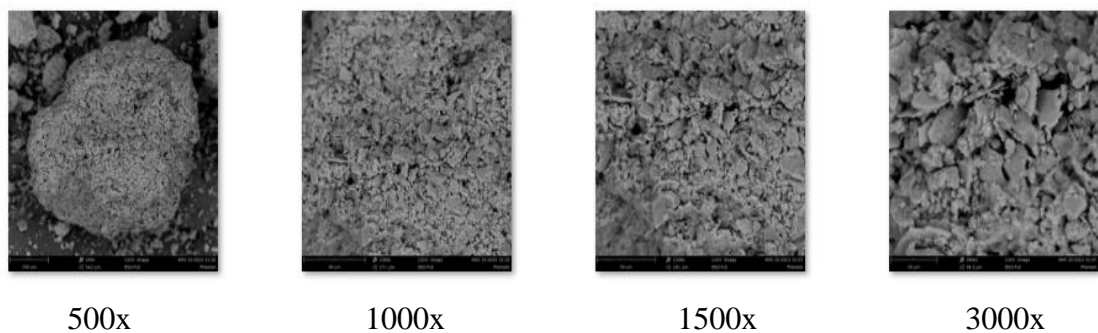


FIGURE 4.4. SEM Micrograph for Raw MK

Figure 4.5a and b and Figure 4.6 a and b shows the observation by using energy dispersive X-ray (EDX) for LFS and MK respectively. Figure 4.5 a and b show the most contributed element in the spotted LFS was calcium and had the least number of Al and

Si. It also had proven in XRF and XRD result that LFS has the highest weight percentage of calcium.

Element	Weight%	Atomic%
C K	16.28	28.04
O K	33.78	43.67
Mg K	1.62	1.38
Al K	1.70	1.30
Si K	7.72	5.68
S K	1.06	0.68
Ca K	35.85	18.50
Fe K	2.00	0.74
Totals	100.00	

FIGURE 4.5a. The elements present in LFS

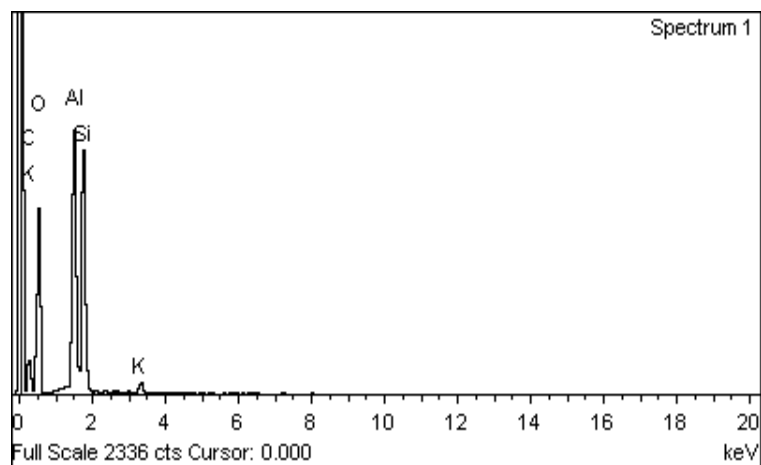


FIGURE 4.5b. The elements present in LFS by graph

From the observation as shown in Figure 4.6a and b for MK, the most spotted element was oxygen. Again it proved the Si and Al ratio in MK were higher than LFS. That's why MK will be the precursor for the geopolymerization process that utilizing the LFS to produce green binder.

Element	Weight%	Atomic%
C K	17.70	25.58
O K	50.07	54.30
Al K	14.69	9.45
Si K	16.58	10.25
K K	0.96	0.42
Totals	100.00	

FIGURE 4.6a. The elements present in MK

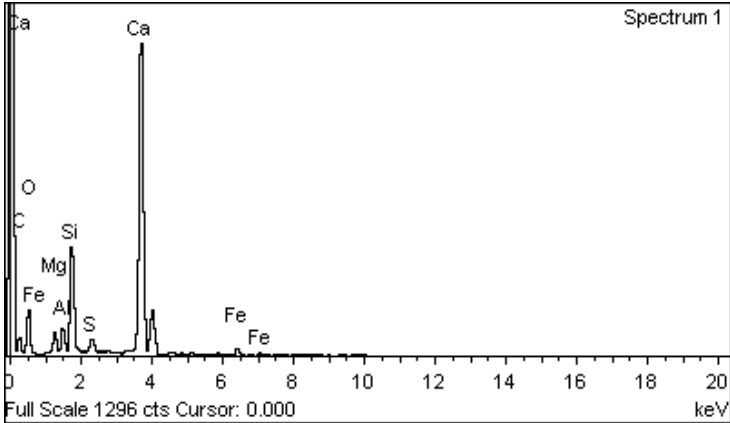


FIGURE 4.6b. The elements present in MK by graph

4.1.4 FTIR Analysis

Figure 4.7 and 4.8 show the FTIR spectra of raw LFS and raw MK respectively.

From Figure 4.7 for raw LFS the peak correspond to portlandite [$\text{Ca}(\text{OH})_2$] which shows the OH- stretching vibration at 3399.4 cm^{-1} . Other than that it correspond to Mg-O bond at 1562.87 and 1466.62 cm^{-1} . The most abundant components are Calcium and the corresponding peaks were at 925.22 and 854.38 cm^{-1} for mayenite and tricalcium aluminate.

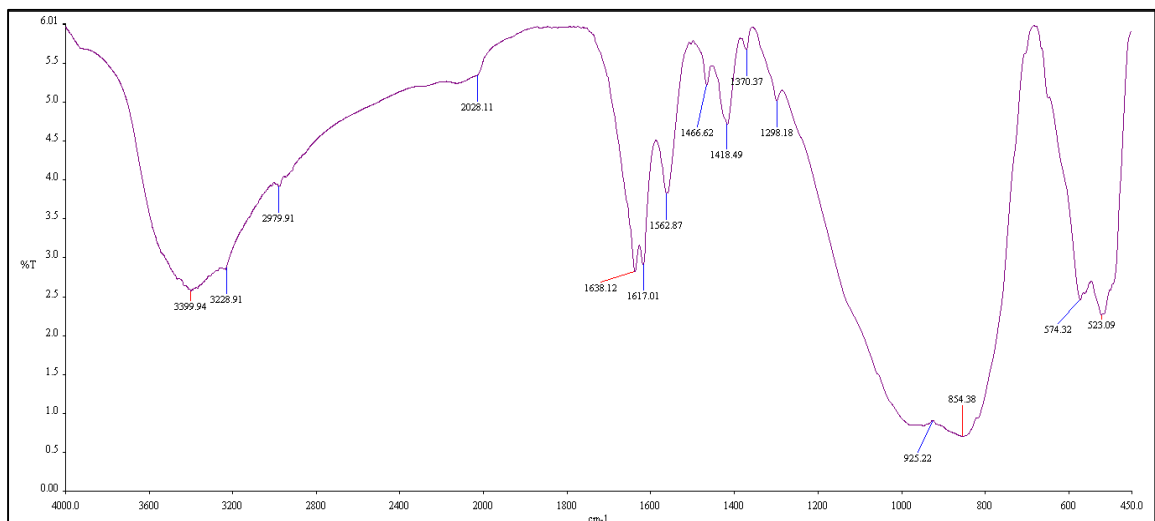


FIGURE 4.7. FTIR analysis for Raw LFS

Referring to Figure 4.8, MK showed characteristic peaks at 3690.76 cm^{-1} and 3619.72 cm^{-1} corresponds to the OH- stretching vibration. H_2O stretching was found at 1628.13 cm^{-1} . Bands at 1030.84 cm^{-1} was assigned to Si-O bonds in the SiO_4 molecules while 796.64 cm^{-1} and 700.64 cm^{-1} were Si-O symmetric stretching.. The other bond at 913.19 cm^{-1} was attributed to $\text{Al}^{\text{IV}}\text{-OH}$ vibration. At 537.06 cm^{-1} was assigned where the Si-O-Al where the Al is in octahedral coordination. All these bonds clearly proved that the main elements present in MK were Si and Al compared to other elements.

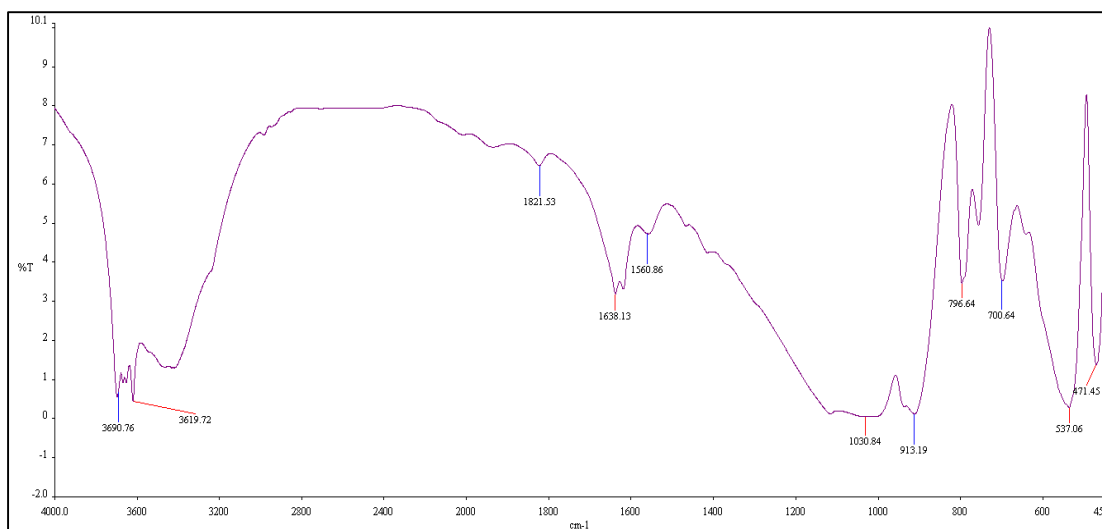
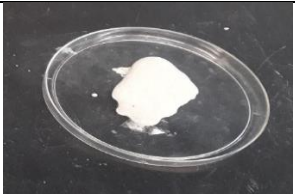

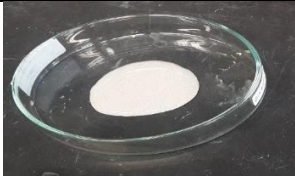
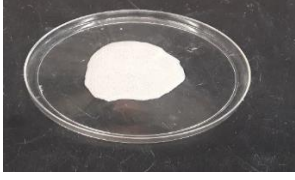
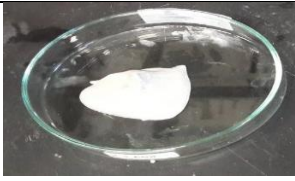


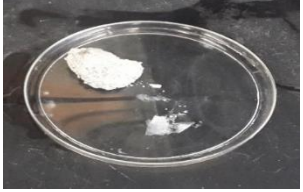

FIGURE 4.8. FTIR analysis for Raw MK

4.2 Determination The Best Solid To Liquid Ratio

As mentioned in methodology, three methods were used to determine the best solid to liquid ratio. Firstly was by mixing the solid which were LFS and MK with liquid activator solution (mixture of NaOH and Na_2SiO_3) and will form homogenous slurry. From the observation in Table 4.2, ratio 1.0 until 1.3 showed that the slurry less viscous, ratio 1.4 showed the slurry mixed so well. However the slurry become too viscous when reach to 1.5 and above.

TABLE 4.2. Solid to Liquid Ratio

Ratio (Solid : Liquid)	Solid (LFS+MK) (g)	Liquid (NaOH+Na ₂ SiO ₃) (g)	Photo
1.0 : 1.0	10	12.5	
1.1 : 1.0	10	10	
1.2 : 1.0	10	8.334	
1.3 : 1.0	10	7.692	
1.4 : 1.0	10	7.143	

1.5 : 1.0	10	6.250	
2.0 : 1.0	10	5.0	

Then, the second test to find the best solid to liquid ratio by porosity test. Concrete that allow water,air,acid and to get through through their tiny holes easily can be said as low porosity concrete. From F. Farhana, et al. (2014) reported that, porosity has more influence on the strength of concrete compared to other parameters. Their researched concluded that the geopolymer paste samples that had the lowest porosity recorded the highest compressive strength.

From the porosity result as shown in Table 4.3, 100% LFS showed the highest porosity and 100% MK recorded the lowest porosity. For different ratios, the porosity did not show much difference among each other. Eventhough , ratio 1.5 show the lowest porosity but from the result of the first experiment by mixing the solid and liquid, this ratio showed that the slurry was less viscous. Therefore the next choice was ratio 1.4. With this combination however, it recorded the second lowest percentage eventhough the slurry were well mixed.

TABLE 4.3. Porosity Result

Solid to Liquid Ratio	Porosity (%)
100 % LFS	54.92
100 % MK	23.67
1.0 : 1.0	37.12
1.1 : 1.0	36.56
1.2 : 1.0	35.98
1.3 : 1.0	35.72
1.4 : 1.0	33.25
1.5 : 1.0	32.03

Table 4.4 showed the results of samples with different solid to liquid ratio for setting time and compressive strength testing.

TABLE 4.4. Detail of mixture proportions

Solid to Liquid Ratio	Amount of solid to liquid in (g)		Setting time (min)	Compressive strength (Mpa)
	Solid(g)	Liquid (g)		
1.0 : 1.0	400	400.00	80	30.04
1.1 : 1.0	400	363.64	75	32.78
1.2 : 1.0	400	333.33	75	34.45
1.3 : 1.0	400	307.69	70	37.33
1.4 : 1.0	400	285.71	60	38.86
1.5 : 1.0	400	266.67	40	33.12

From the results illustrated in Figure 4.9, it was observed that the setting time decreased when the solid to liquid ratio increased. The compressive strength on the other hand increased when the solid to liquid ratio increased but suddenly decreased when it reached ratio 1.5. At solid to liquid ratio 1.4, it recorded the optimum compressive strength which was 38.86 MPa.

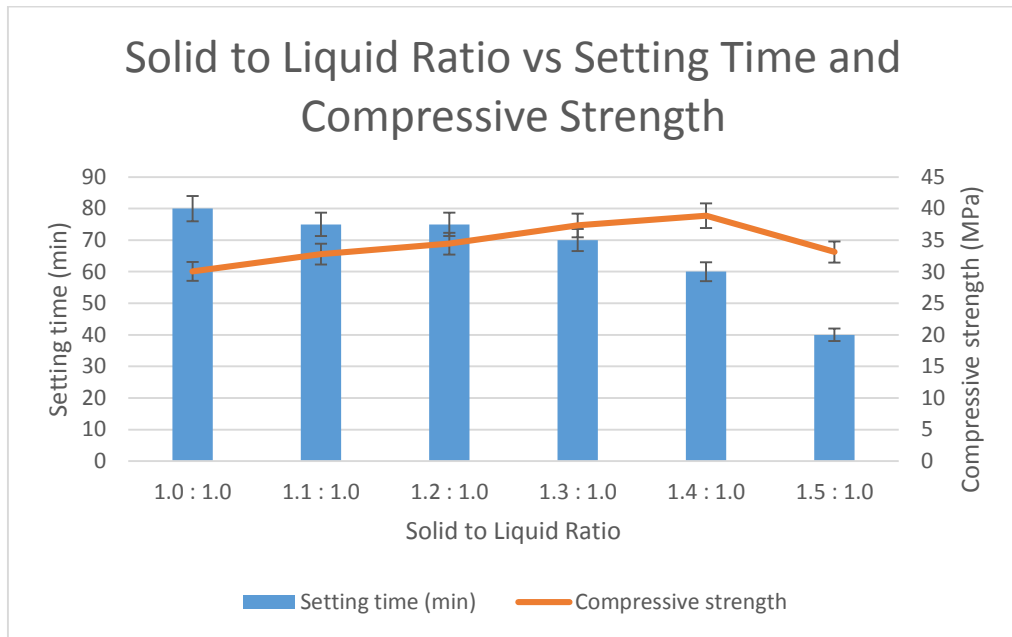


FIGURE 4.9. Solid to Liquid Ratio vs Setting Time and Compressive Strength

From all of results it was found that solid to liquid ratio 1.4 showed the slurry was well mixed, recorded second lowest porosity and the highest compressive strength. So, the solid to liquid ratio of 1.4 had been chosen for the next step of the study.

4.3 Experimental Result

After three test were carried out to find solid to liquid ratio, finally best solid to liquid ratio determined was 1.4:1.0. By fixing the ratio, now the research proceed by varying the composition of LFS and MK. The mix design of the investigated samples were reported in Table 3.4.

4.3.1 X-Ray Diffraction (XRD)

Mineralogical analysis were carried out by X-Ray diffractometer with Cu K α radiation in the 5-80 $^{\circ}$ 2 θ range. XRD patterns of raw LFS and raw MK were reported in Figure 4.1 and 4.2 respectively. Figure 4.10 illustrates the comparison of the XRD results of raw LFS and raw MK with geopolymer samples which were G-MK 100, G-LFS 100 G-25:75, G-50:50 and G-75:25 and G-LFS 100.

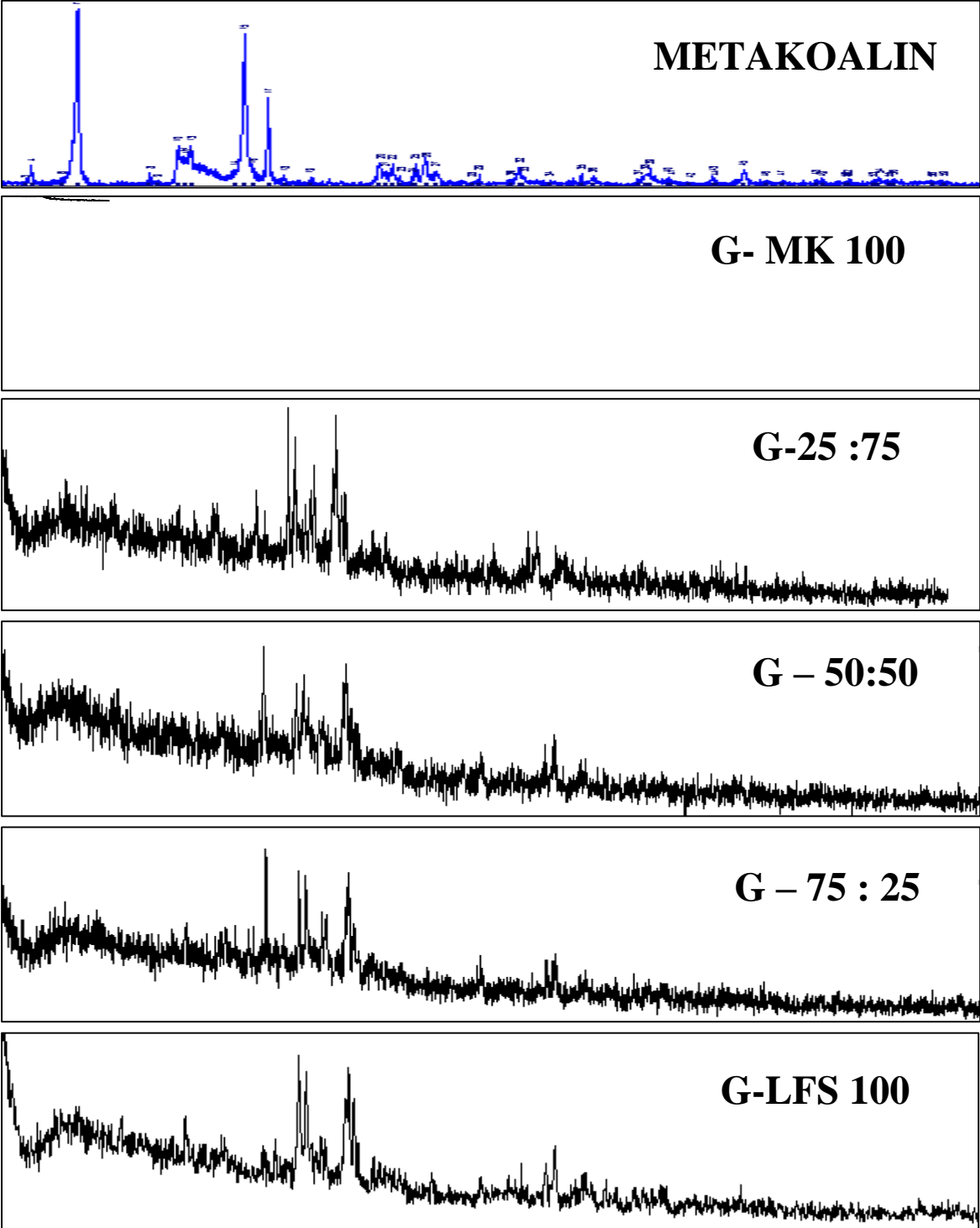
Kaolin will be transformed to MK after calcined. The XRD pattern of calcined kaolin shows amorphous pattern. However, there are still kaolinite peaks [Al₂(Si₂O₅)(OH)₄] that showed calcination process was not complete. Quartz [SiO₂] and Muscovite [(K,Na)(Al,Mg,Fe)₂(Si_{3.1}Al_{0.9})O₁₀(OH)₂] were largely unreactive and remained in the MK.

After geopolymerization occur, XRD of G- MK100 showed that the quartz and kalonite started to disappear except Muscovite which act as an amorphous structure while zeolite starts to appear. The introduction of LFS with different composition in geopolymerization process modifies the XRD pattern.

The explanation about XRD pattern for raw LFS had been discussed at section 4.1. As mentioned, the major compound presents are calcium silicates (with or without small quantities of aluminium or magnesium) such as Diopside (CaMgSi₂O₆) and olivine (Ca₂SiO₄). Aluminates such as spinel was present due to alumina contents in the slag. Other significant phase was perovskite (CaTiO₃), periclase (MgO) and iron oxide (Fe_xO_y). Ladle slag showed cementitious property mainly in the presence of an alkaline activator. The compound present in G-LFS 100 were calcium aluminium silicate hydrates (CaAl₂Si₇O_{18.5}H₂O), yugmaralite (Ca₄Al₇Si₂₀O₁₈) and heulandite (CaAl₂Si₇O_{18.6}H₂O).

When comparing the XRD pattern for every geopolymer samples with decreasing LFS content, peaks at 30-35 2 θ become less evident and the hump move towards the values observed for G-MK100 whereas increasing LFS content will move the humps toward the values observed for G-LFS 100. XRD of MK displays a broad hump at 22 $^{\circ}$ 2 θ . In G-MK 100 traces of MK peak was still evident, whereas they completely disappear by adding LFS, thus confirming an interaction between LFS and MK during the

consolidation process in LFS based materials. This result showed the similar findings as reported by M.C Bignozzi, et al. (2012) as per discussed in section 2.3.2.



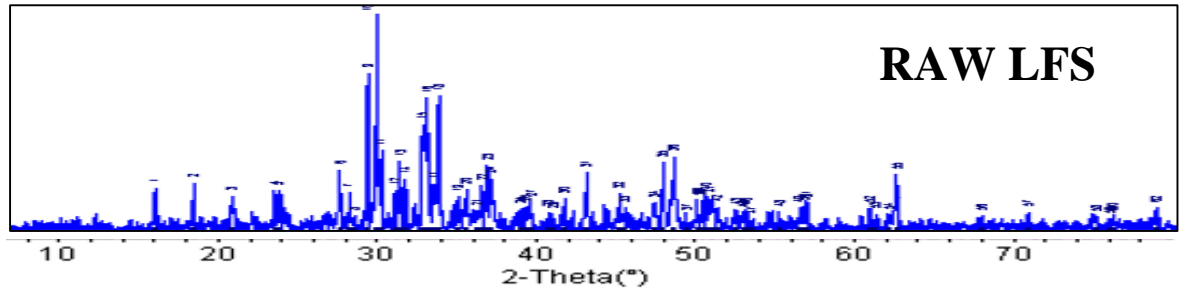
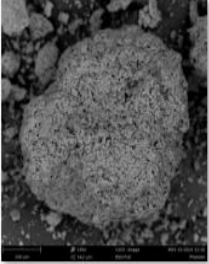
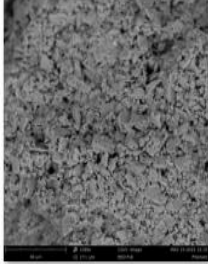
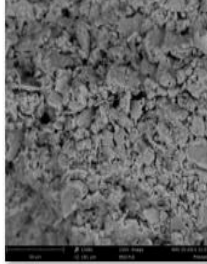
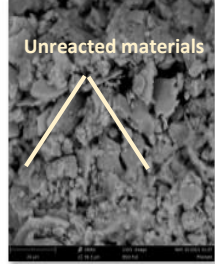
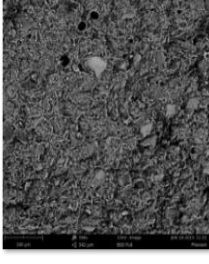
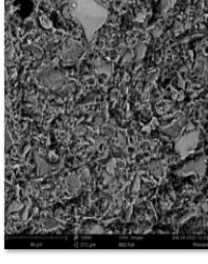
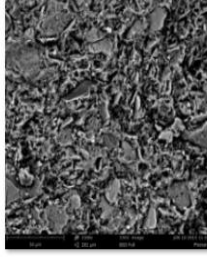
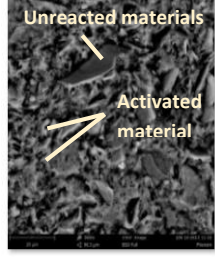
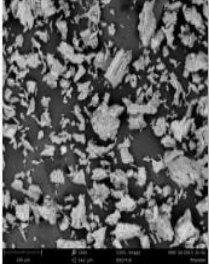
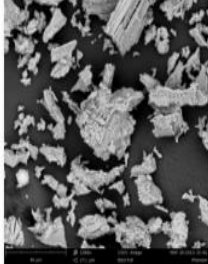
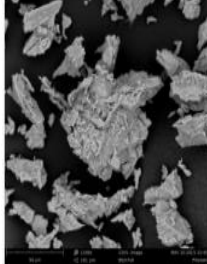
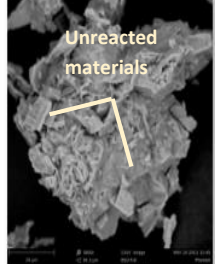
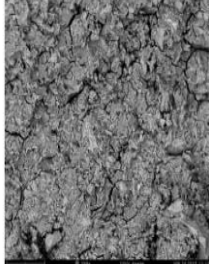
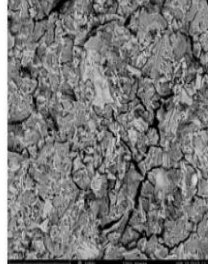
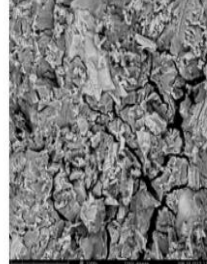
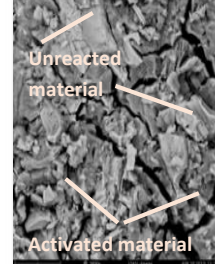


FIGURE 4.10. XRD Pattern of Raw MK, G-MK100, G-25:75, G-50:50, G-75:25, G-LFS 100 and Raw LFS

4.3.2 Morphological

Figure 4.11 display the comparison of SEM micrograph between raw materials and hardened paste geopolymer. Raw MK and raw LFS 100% showed the unreacted materials. After raw materials reacted with alkali activated materials, the geopolymerization process occur. After geopolymerization occur, unreacted materials convert to activated materials for G-MK 100, G-LFS 100, G-75:25 and G-50:50. For LFS, a cracked structure was observed and thus contributed to the lowest compressive strength. This cracked structure can be considered as same as what had been observed by M.C.Bignozzi et al.(2012) which explained as with increasing LFS content, which particles are visible as white dots in SEM micrograph, there is a correspondent increase of gel and structure heterogeneity as per discussed in section 2.3.3. M.C.Bignozzi et al.(2012) also said that with increasing the LFS content, the large pores and low compressive strength detected for G-LFS100 was due to the formed microstructure appearing much less homogenous than those shown by LFS/MK.

When comparing between G-50:50 and G-75:25, it can be seen that less unreacted particles could be observed in G-50:50 instead of to G-75:25. This contributed to highest compressive strength. This proved that water takes part in dissolution, hydrolysis and polycondensation reaction during geopolymerization as it provided a medium for the dissolution of alumino-silicates and the transportation of various ions, hydrolysis of Al^{3+} and Si^{4+} compounds and polycondensation of different aluminate- and silicate-hydroxyl species. This brings to the continuous dissolution of residual solid particles and hydrolysis of generated Al^{3+} and Si^{4+} to form homogenous structure (Zuhua, 2009)

Raw MK				
G-MK 100				
Raw LFS				
G-LFS 100				

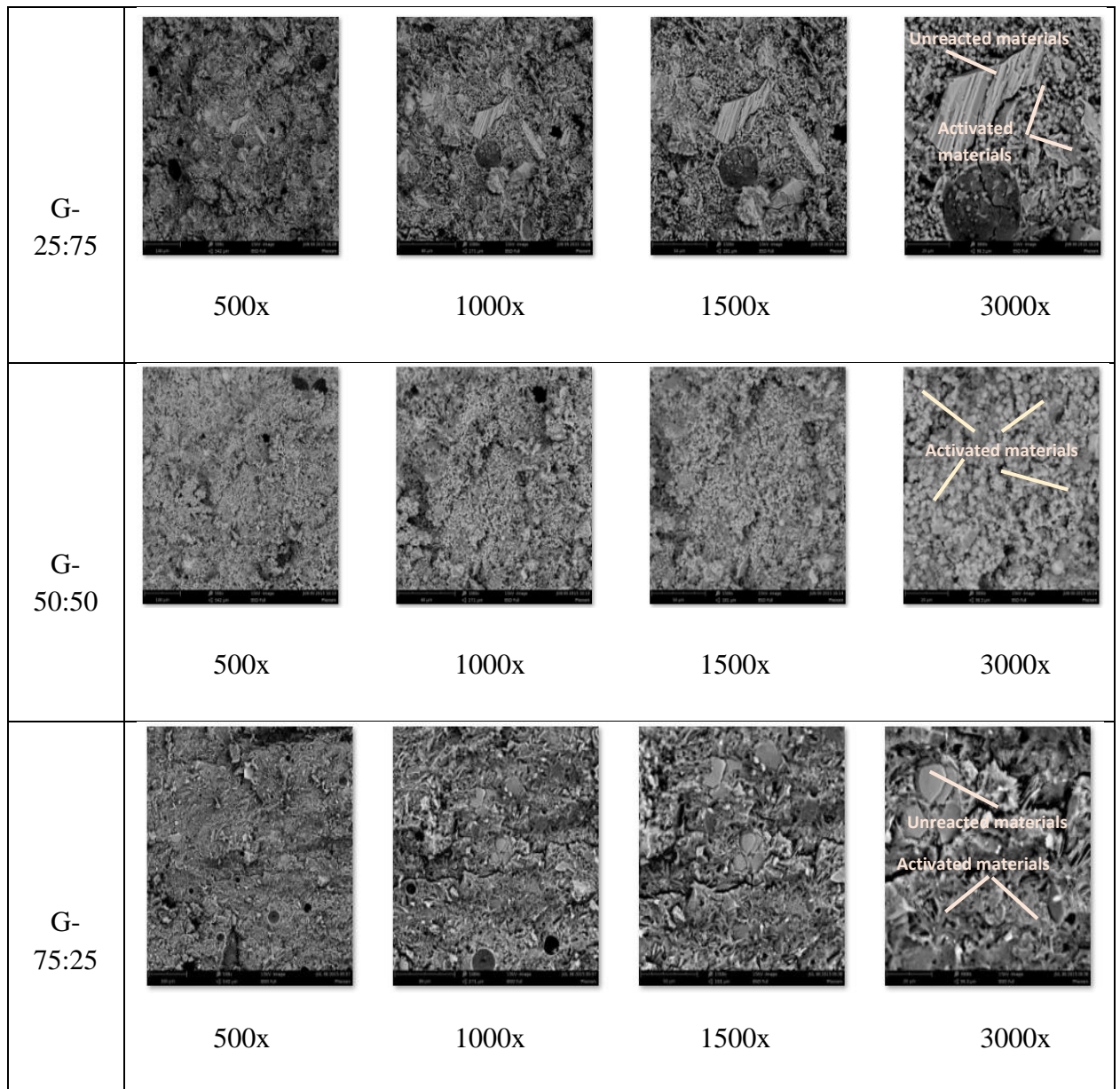

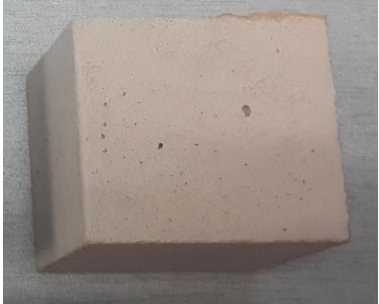


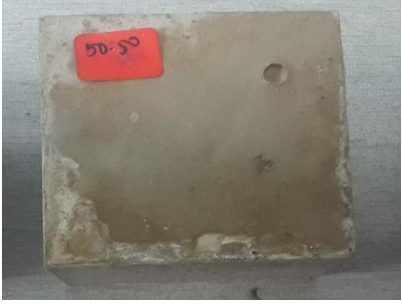

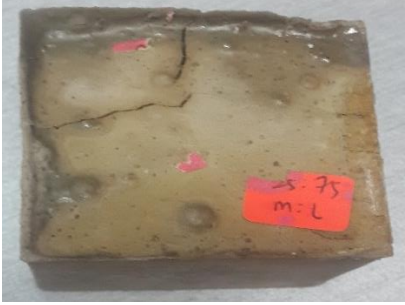

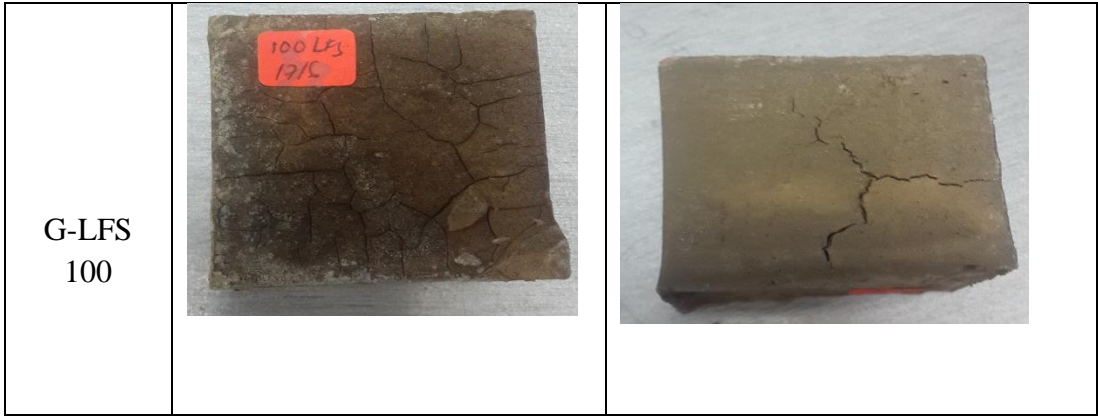


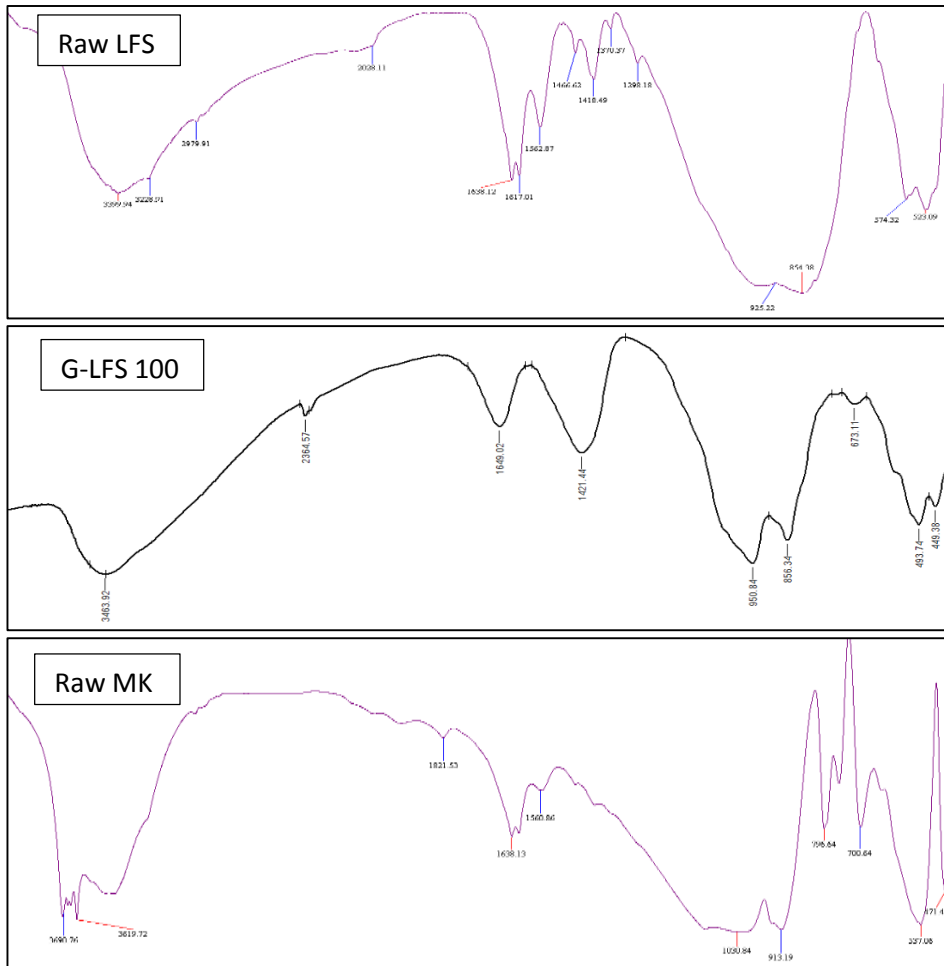
FIGURE 4.11. Comparison of SEM Micrographs between Raw MK, G-MK100, G-25:75, G-50:50, G-75:25, G-LFS 100 and Raw LFS

TABLE 4.5. Structure of samples (Front and back view)

SAMPLE	FRONT	BACK
G-MK 100		
G-25:75		
G-50:50		
G-75:25		



4.3.3 FTIR Analysis



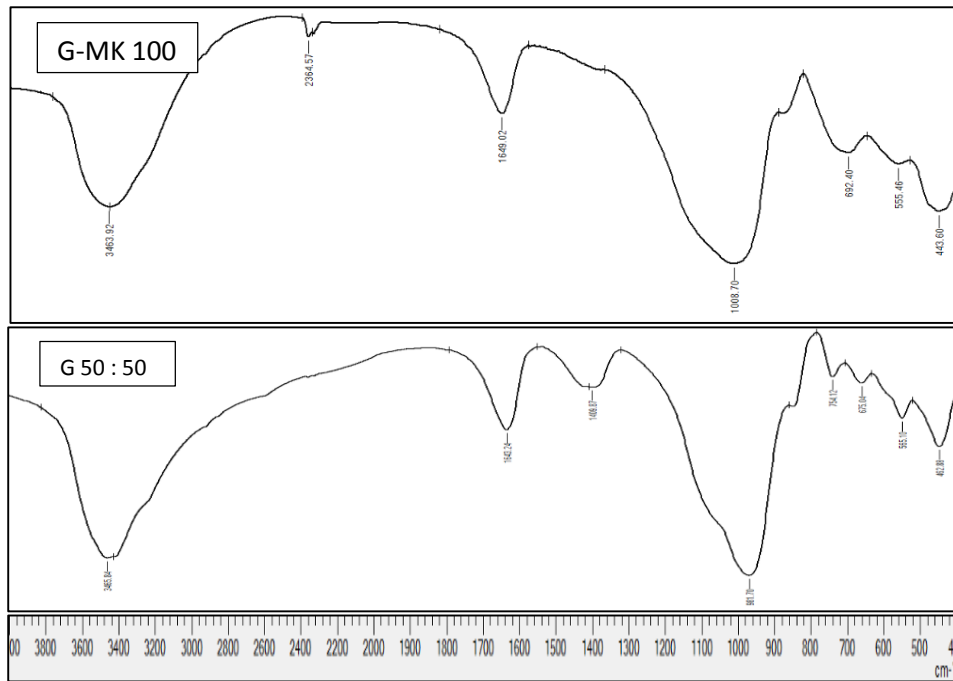


FIGURE 4.12. Comparison of FTIR analysis between Raw LFS, G-LFS 100, Raw MK, G-MK100 and G-50:50

TABLE 4.6. Summary of main FTIR peak

Bonds	Raw MK	Raw LFS	G-MK 100	G-LFS 100	G-50:50
OH ⁻	3690.76 3619.72	3399.4	3465.92	3463.92	3465.84
H ₂ O	1638.13	1638.12	1649.02	1649.02	1643.24
Mg-O		1562.87 1466.62			
Al-O/Si-O		1418.49	1409.87	1421.44	1409.87
Si-O	1030.84				
Si-O-T (T=Al or Si)			1008.07	950.84	981.70
Ca-Al-O		925.22 854.38		856.34	

Al ^{IV} -OH					
Si-O	796.64				
Al-O					
Si-O-T (T=Al or Si)					754.12
Si-O	700.64				
Zeolite			692.40	673.11	675.04
Si-O-Al ^{IV}			555.46		565.10
Ca-Al-O	537.06	574.32 523.09			

Figure 4.12 showed the comparison of FTIR analysis between Raw LFS, G-LFS 100, Raw MK, G-MK100 and G-50:50. The result from raw material especially raw MK, showed that the broad band was observed at 3690.76 and 3619.72 cm⁻¹ (OH⁻ vibration). The intensity decreased which resulted in hardened paste of geopolymer in all G-MK 100, G-LFS 100 and G 50:50. This meant that there were large amount of water absorbed into the surface of the geopolymer structure and was expelled out from the structure after the curing process to form cement paste.

The same observation corresponded to H₂O bond which increased from raw material to geopolymer hardened paste. This addition of water was purposely conducted for the continuous dissolution of raw materials and the hydrolysis and polycondensation process, and was expelled out from the structure after curing. The band between 1390 to 1430 cm⁻¹ represent the asymmetrical stretching vibrations of Al-O and Si-O bonds. Si-O-T linkages occurred at 1030.84 cm⁻¹ shifted to lower frequency at 1008.07 , 950.84 and 981.70 cm⁻¹ which represent G-MK 100 , G-LFS 100 and G-50:50 respectively. This indicated that there was probably changes in the silicate network whereby there was increasing of non-bridging oxygen in silicate sites and the increasing of Al substitution in the silicate network as suggested by Mohammadi, Provis & Deventer (2008). These

peaks showed an increase in intensity from raw calcined metakaolin into hardened paste geopolymer suggesting that the geopolymerization process continued after the addition of water into the raw materials. Another new peak only present at G- 50:50 which was 754.12cm^{-1} represent symmetrical vibration of Si-O-T bonding of AlO_4 and SiO_4 tetrahedrons. This again was the proof the geopolymerization. In the resulted hardened paste, the zeolite peak was found at 675.04 cm^{-1} which were also observable in the XRD pattern.

However for LFS, there were extra peaks which represent the Mg-O bonding at 1562.87 and 1466.62 cm^{-1} . Other than that, Ca-O-Al bonds were found present at 925.22 , 854.38 , 574.32 and 523.09 cm^{-1} . These identified calcium are the most abundant components in LFS.

4.4 Physical Properties Of Geopolymer

4.4.1 Setting Time and Compressive Strength

TABLE 4.7. Setting time and compressive strength result

	Setting time (min)	Compressive strength (MPa)		
		7days	14 days	28 days
G- MK 100	50	40.85	46.08	48.24
G-25:75	45	15.56	46.97	50.11
G-50:50	60	34.25	48.49	54.06
G-75:25	65	43.44	37.16	35.79
G-LFS 100	300	4.52	10.07	33.80

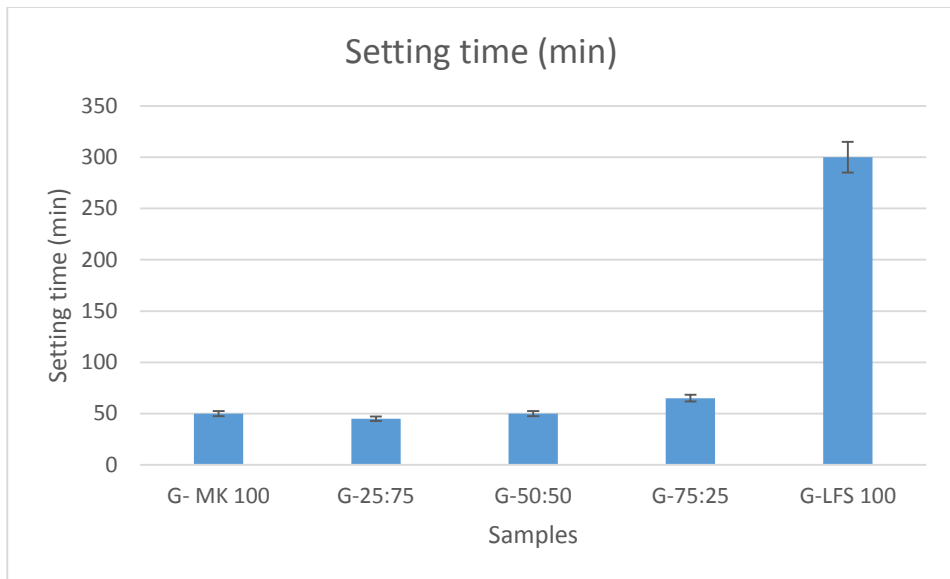


FIGURE 4.13. Setting time of samples prepared

As mentioned in 2.4.2 by Moulin, et. Al (2001), a good binder should come with slower setting time for a more convenient period of workability for the application in construction/ buildings. From the observation, when LFS content was higher in the composition, the setting time will increase. And from two contradict research as per discussed in 2.4.2, after carried out the experiment Moulin, et. Al (2001) findings was suited to this project that present of MK was to shorten the setting times compared to other sample especially the control samples not longer the setting time as found by Pantazopoulou, et al. (2004). From Figure 4.13, G-LFS 100 recorded the slowest time to set which was 300min. Although the target of this research was to find the binder with the slowest setting time, but G-LFS 100 and G-75:25 recorded the lowest compressive strength. So the best ratio of LFS to MK was G-50:50 because it recorded the highest compressive strength and recorded the lowest setting time which was 60 minutes.

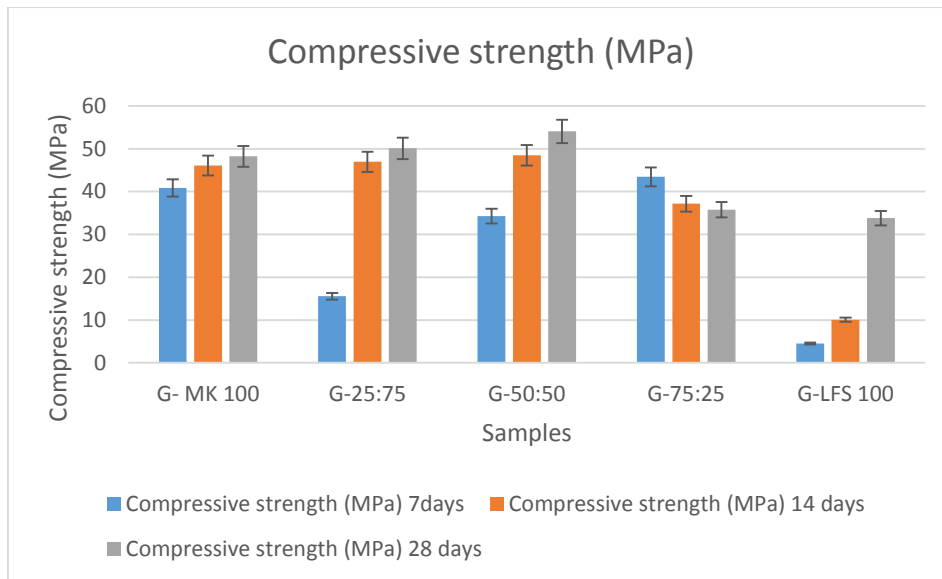


FIGURE 4.14. Compressive strength of samples prepared

Utilizing MK as precursor showed positive result for geopolymerization process. Compressive strength test had been carried out. From Figure 4.14 for raw material, strength between G-MK100 and G-LFS 100 showed a biggest difference at 48.24 and 20.80 MPa respectively while when varying the composition, G-50:50 showed the highest strength followed by G-25:75 and G-75:25. This can be related with the Fernandez-Jimenez, et al. (2005) study which that silica plays a main role in geopolymerization for making strong bonds. Many researchers agree that the strength of material is enhanced by increasing the Si ratio, but after getting optimum compressive strength additional silica in the matrix causes reduction in strength. So the research from (Bignozzi, et al. 2012) was not valid whereby it was mentioned that by increasing the LFS content and decreasing the MK will reduce the compressive strength. It had been proved in this study that with the increase of LFS content, compressive strength decreased in the range of 20-36MPa compared to MK that show higher compressive strength. The particle size also can be one of the reasons for the compressive strength because smaller size of MK compared to LFS leads to higher dissolution of raw materials with alkaline solutions and give a greater compressive strength.

4.4.2 Porosity Test

Porosity also effects the compressive strength. When porosity decreased, the pore size also decreased. As a result, it would be expected that the compressive strength will increased when the porosity is decreased. From Table 4.8 and Figure 4.15, the compressive strength increased from day 7 until 28. This is because the structure of samples becomes denser, harder and improved crystallinity from day 7 until day 28. The pore size decreases and the atoms are closer to each other. The porosity and permeability also decreased hence the durability and workability would be improved. This results was the similar as reported by F. Farhana, et al. (2014) that when comparing the compressive strength between day 7 and day 90, the compressive strength at day 90 are higher with lowest porosity.

TABLE 4.8. Porosity result

Samples	Porosity		
	7 days	14 days	28days
G- MK 100	27.19	21.03	20.30
G-25:75	26.38	25.92	20.89
G-50:50	30.31	26.03	23.15
G-75:25	47.93	43.08	38.83
G-LFS 100	37.18	36.28	36.09

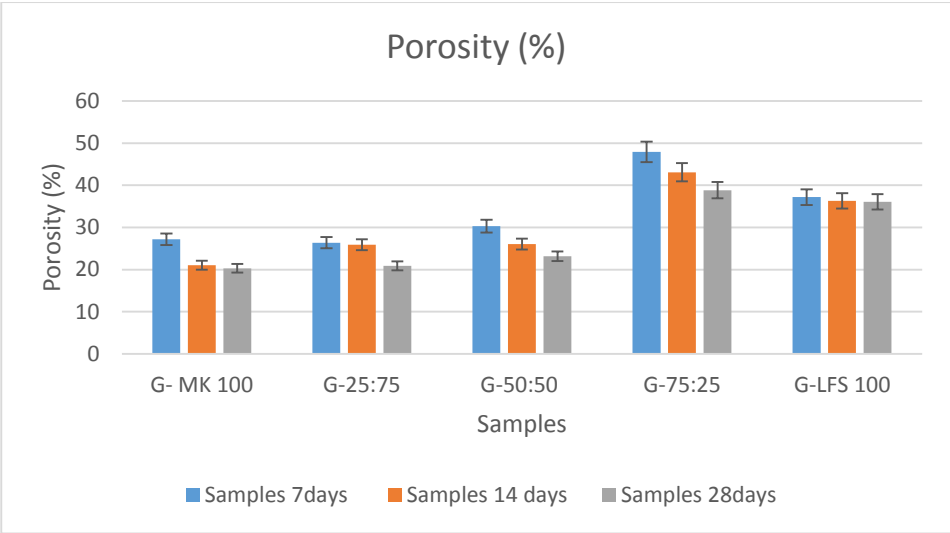


FIGURE 4.15. Porosity test

4.4.3 Degree of Reaction

From Table 4.9 and Figure 4.16, G-50:50 showed the highest degree of reaction while G-LFS 100 showed the lowest degree of reaction. This is proportional to the compressive strength result and inversely proportional to porosity test. When porosity decreased, the compressive strength will be increase together with the degree of reaction.

TABLE 4.9. Degree of reaction (%)

Samples	Degree of reaction (%)		
	7 days	14 days	28 days
G- MK 100	83.91	86.18	88.15
G-25:75	93.75	94.80	95.21
G-50:50	93.60	94.50	97.59
G-75:25	72.26	79.81	76.35
G-LFS 100	66.53	69.86	71.98

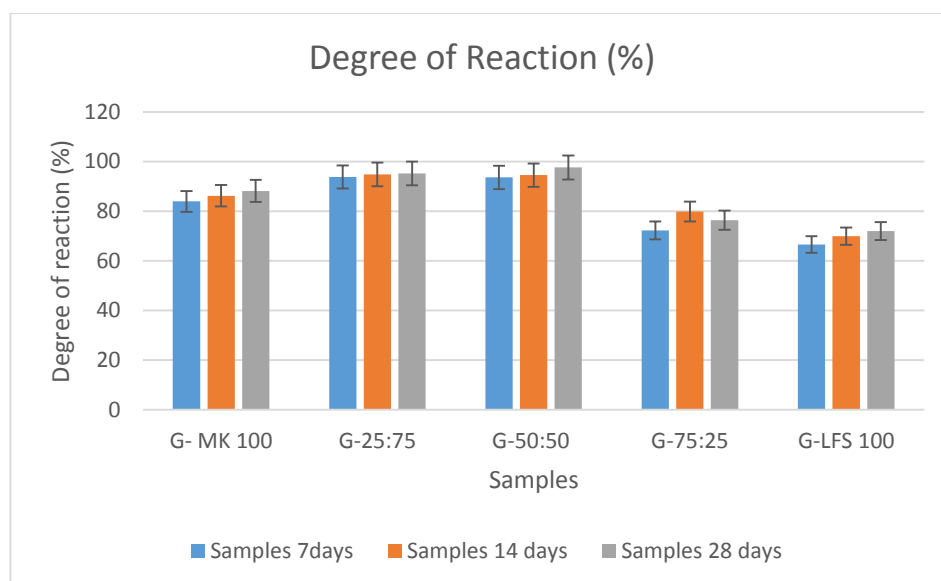


FIGURE 4.16. Degree of reaction

CHAPTER 5

CONCLUSION AND RECOMMENDATIONS

5.1 Conclusion

The results of this research can be summarized as follows:

LFS has beneficial properties such as good strength, durability and pozzolonic properties that can be utilized in many engineering applications such as road construction, soil stabilization and binder in concrete. To become a binder, LFS should be mixed with MK as a precursor and AAM through geopolymerization reaction due to low content of Si and Al ratio. By fixing solid to liquid ratio which is 1.4, curing temperature at 60°C and concentration of NaOH (8M), the best composition for binder was produced at 50:50 ratio of LFS and MK(G-50:50) with a consistent high compressive strength and slower setting time for a more convenient period of workability for application in construction / buildings.

Results from XRF, XRD and SEM for raw materials before geopolymerization take place, had proved that LFS had low content of Si and Al but high content of CaO compared to MK. After geopolymerization process take place the XRD result showed that when LFS content is decreased, the peaks at 30-35 2 θ become less evident and the hump moves towards the values observed for G-MK 100. This shows the positive interaction between LFS and MK. For SEM, before geopolymerization takes place, the raw data shows 100% unreacted materials. However when geopolymerization take place, the unreacted materials will be converted to activated materials and G-50:50 showed that almost 100% unreacted materials had been converted to activated materials. For the structure, when increasing LFS content increases, there were showed that some cracking structure at the surface of samples was observed compared to high content of MK. This will lead to lower

compressive strength. G-50:50 shows the best structure without any cracking present. For FTIR result, OH⁻ vibration that clearly observed at 3690.76 and 3619.72cm⁻¹ for raw material, the intensity decreased after geopolymerization takes place. This is due to large amount of water absorbed into the surface of geopolymer structure and expelled out from the structure after curing process to form cement paste.

Compressive strength strongly influences the open porosity and particle size distribution. LFS has bigger particle size compared to MK. Thus, the hardened geopolymer which has high content of LFS will have higher porosity and lower compressive strength. Addition of MK was found to improve compressive strength until the optimum level which was after which it reduces. For the setting time, a good binder will come with slowest setting time but highest compressive strength. G-50:50 recorded the one of the slowest setting time with the highest compressive strength. For degree of reaction, G-50:50 recorded the highest degree of reaction compared to other samples. When comparing from day 7, 14 and 28 days, G-50:50 showed the highest compressive strength and degree of reaction which were 54.06MPa and 97.59% after 28 days respectively.

5.2 Recommendations

For further research of the project, it would be best if a detail study is carried out on the process of geopolymerization. It is suggested that the discussed parameters are measured at wider range to observe the effect on the kinetics of geopolymerization. It is also suggested that to vary other parameters such as concentration of NaOH or curing temperature because different concentration and curing temperature will show different results. Other than that, instead of using metakaolin, try to use fly ash, rice husk ash or palm ash in order to find the best reaction since they also have high content of Si/Al that can also be precursor to the geopolymerization process. The addition of samples tested under each parameter discussed would generate more accurate results on the study.

REFERENCES

- A. Elimbi, H. T. (2011). Effects of calcination temperature of kaolinite clays on properties of geopolymer cements. *Construction and Building Materials*, 25(6), 2805-2812.
- A.M Mustafa Al Bakri, H. M. (2014). Mechanism and Chemical Reaction of Fly Ash Geopolymer Cement. *Journal of Asian Scientific Research*, 1(5), 247-253.
- A.Natali Murri, W. R. (2013). High temperature behaviour of ambient cured alkali-activated materials based on ladle slag. *Cement and Concrete Research*, 43, 51-61.
- Afshan Asif, Z. M. (2014). *Effect of NaOH concentration on the strength of non sodium silicate fly ash geopolymer*. Perak, Malaysia: Department of Chemical Engineering, Universiti Teknologi PETRONAS.
- Ankica Radenovic, J. M. (2013). Characterization of Ladle Furnace Slag from Carbon Steel Production as a Potential Adsorbent. *Advances in Materials Science and Engineering*, 2013, 6.
- Bing-hui Mo, H. Z.-m. (2014). Effect of curing temperature on geopolymerization of metakaolin based geopolymer. *Applied Clay Science*, 144-148.
- Btis G. Pantazopoulou P, T. S. (2004). The effect of metakaolin on the corrosion behaviour of cement mortars. *Cement and Concrete Composites*.
- Bui Dang Trung, D. V. (2009). Recent research geopolymer concrete. *The 3rd ACF International Conference*. ACF/VCA. Retrieved from <http://www.sciencedirect.com/science/article/pii/S0304389406002081>
- Caijun Shi, S. H. (2003). Cementitious properties of ladle slag fines under autoclave curing conditions. *Cement and Concrete Research* , 33, 1851-1856.
- Davidovits, J. (1999). Chemistry of geopolymeric systems. *In Proceedings Second International Conference, Geopolymer* (pp. 9-39). France: Geopolymer Institute.
- Eric Maoulin, B. P. (2001). Influence of key cement chemical parameters on the properties of metakaolin blended cement. *Cement and Concrete Composites*, 23(6), 463-469.

- Farah Farhana, H. K. (2014). A Study on Relationship between Porosity and Compressive Strength for Geopolymer Paste. *Kay Engineering Materials*, 594-595, 1112-1116.
- Fernandez-Jimenez, A. A. (2005). Composition and microstructure of alkali activated fly ash binder:effect of the activator. *Cement and concrete research*, 35(10), 1984-1992.
- Hajimohammadi, A. J. (2008). One-part geopolymer mixes from geothermal silica and sodium aluminate. *Am Chem Socciate*, 47, 9396–9405.
- Hua Xu, J. S. (2004). Effect of Source Materials on Geopolymerization. *Industrial and Chemistry Research*, 16-98-1706.
- Hua Xu, J. V. (2000). The geopolymerisation of alumino-silicate minerals. *International Journal of Mineral Processing* 59, 247-266.
- Irem Zaynep Yildirim, M. P. (2011). Chemical,Mineralogical and Morphological Properties of Steel Slag. *Advances in Civil Engineering*, 2011, 13.
- Isabella Lancellotti, C. P. (2014). Incinerator Bottom Ash and Ladle Slag for Geopolymers Preparation. *Waste Biomass Valor*, 5, 393-401.
- J. Temuujin, R. W. (2009). Effect of mechanical activation of fly ash on the properties of geopolymer cured at ambient temperature. *Journal of Materials Processing Technology*, 209(12-13), 5276-5280.
- Kostas Komnitsas, D. Z. (2007). Geopolymerisation : A review and prospects for the mineral industry. *Mineral Engineering*, 1261-1277.
- L. Adreas, S. D. (2014). Steel slags in a landfill top cover. *Waste Management*, 34(3), 629-701.
- Maria Chiara Bignozzi, S. M. (2012). *Mix-Design and chararacterization of alkali activated materials based on metakaolin and ladle slag*. Retrieved from Applied Clay Science: <http://www.sciencedirect.com/science/article/pii/S0169131712002323#>
- Nath, P. &. (2012). Geopolymer concrete for ambient curing condition. *Australasian Structural Engineering Conference*.

- Norbaizurah Rahman, A. K. (2014). Investigation on the Degree of Reaction and Strength Performance of Fly Ash Based Geopolymer Binder. *Material Science*.
- P.Duxson, A.-J. J. (2006). *Geopolymer technology : the current state of the art*. Advances in Geopolymer Science & Technology.
- Ppayiani, E. (2013). *Utilization of electric furnace arc steel slags in concrete products*. Greece: Department of Civil Engineering, Aristotle University of Thessaloniki.
- Prinya Chindaprasirt, C. J. (2009). Comparative study on the characteristics of fly ash and bottom ash geopolymers. *Waste management*, 29(2), 539-543.
- S.Alonso, A. (2001). Alkaline activation of metakaolin and calcium hydroxide mixtures : influence of temperature, activator concentration and solid ratio. *Materials Letters*, 47(1-2), 55-62.
- The Concrete Society Your Concrete Community*. (n.d.). Retrieved from Alkali activated cements (including geopolymer cements): <http://www.concrete.org.uk/fingertips-nuggets.asp?cmd=display&id=902>
- Y.M Liew, H. K. (2012). Processing and Characterization of Calcined Kaolin Cement Powder. *Construction and Building Materials*, 794-802.
- Zuhua, Z. (2009). Role of water in the synthesis of calcined kaolin-based geopolymer. *Appl Clay Science*, 43, 218 -223.